2-23-2010

Requirements for Transitional Endoplasmic Reticulum Site Structure and Function in Saccharomyces cerevisiae

Polina Shindiapina
Dartmouth College

Charles Barlowe
Dartmouth College

Molecular Biology of the Cell
Vol. 21, 1530–1545, May 1, 2010

Requirements for Transitional Endoplasmic Reticulum Site Structure and Function in *Saccharomyces cerevisiae*

Polina Shindiapina and Charles Barlowe

Department of Biochemistry, Dartmouth Medical School, Hanover, NH 03755

Submitted July 23, 2009; Revised February 22, 2010; Accepted February 23, 2010
Monitoring Editor: Benjamin S. Glick

Secretory proteins are exported from the endoplasmic reticulum (ER) at specialized regions known as the transitional ER (tER). Coat protein complex II (COPII) proteins are enriched at tER sites, although the mechanisms underlying tER site assembly and maintenance are not understood. Here, we investigated the dynamic properties of tER sites in *Saccharomyces cerevisiae* and probed protein and lipid requirements for tER site structure and function. Thermosensitive *sec12* and *sec16* mutations caused a collapse of tER sites in a manner that depended on nascent secretory cargo. Continual fatty acid synthesis was required for ER export and for normal tER site structure, whereas inhibition of sterol and ceramide synthesis produced minor effects. An in vitro assay to monitor assembly of Sec23p-green fluorescent protein at tER sites was established to directly test requirements. tER sites remained active for ~10 min in vitro and depended on Sec12p function. Bulk phospholipids were also required for tER site structure and function in vitro, whereas depletion of phophatidylinositol selectively inhibited coat protein complex II (COPII) budding but not assembly of tER site structures. These results indicate that tER sites persist through relatively stringent treatments in which COPII budding was strongly inhibited. We propose that tER site structures are stable elements that are assembled on an underlying protein and lipid scaffold.

INTRODUCTION

The biogenesis of secretory proteins is initiated at the endoplasmic reticulum (ER) where nascent polypeptides are translated, folded, and then transported forward in membrane-bound carrier vesicles. Formation of transport vesicles from the ER is catalyzed by the COPII complex, which is assembled on the ER surface by sequential recruitment of the Sar1p GTPase, followed by the Sec23/24 complex and finally the Sec13/31 complex (Lee *et al*., 2004). Secretory cargo are selected into COPII vesicles through activity of the Sec23/24 adaptor complex (Kuehn *et al*., 1998; Miller *et al*., 2003; Mossessova *et al*., 2003), whereas polymerization of the outer layer Sec13/31 cage structure deforms ER membranes to produce COPII-coated transport vesicles (Matsuoka *et al*., 2001; Stagg *et al*., 2006).

Morphological studies have revealed that COPII proteins are not distributed uniformly on the surface of the ER but instead are organized into distinct subdomains, known as transitional ER (tER) sites, where nascent secretory cargo is exported (Orci *et al*., 1991; Bannykh *et al*., 1996; Rossanese *et al*., 1999). Live cell imaging shows that tER sites are dynamic structures, although individual tER sites can be monitored and are stable on the order of several minutes (Stephens *et al*., 2000; Hammond and Glick 2000; Bevis *et al*., 2002). In contrast, experimental evidence indicates that turnover of single COPII subunits at tER sites is on the order of 1–4 s (Forster *et al*., 2006). Additional tER site components, including the large peripherally associated Sec16 protein, are thought to assemble into scaffolds that stabilize transitional ER zones (Connerly *et al*., 2005; Watson *et al*., 2006; Bhattacharyya and Glick 2007). Recent studies have shown that changes in the level of secretory cargo synthesis and membrane lipid composition can influence tER site dynamics and the total number of tER sites per cell (Forster *et al*., 2006; Runz *et al*., 2006; Farhan *et al*., 2008). However, the molecular mechanisms that govern tER site structure and function are largely unknown.

Organized tER sites have been observed across several species and in many instances are positioned adjacent to Golgi elements (Rossanese *et al*., 1999; Kondylis and Rabouille, 2003; Yang *et al*., 2005). However, in the yeast *Saccharomyces cerevisiae*, fluorescence microscopy documents that COPII proteins localize to smaller puncta that are continuous with the ER but have no apparent orientation to dispersed Golgi compartments (Rossanese *et al*., 1999). Here, we characterize these smaller COPII puncta and find that these sites are relatively long lived (up to 4 min) and display similar properties as described for mammalian tER sites. To gain basic insight into the protein and lipid requirements for tER site assembly, we have examined the influence of specific mutations and inhibitors on tER site structure and function in *S. cerevisiae* by using in vivo and cell-free approaches.

MATERIALS AND METHODS

Materials

Cerulenin and phosphatidylcholine (PC)-phospholipase C (PLC) were purchased from Sigma-Aldrich (St. Louis, MO). Phosphatidylinositol (PI)-PLC was purchased from Invitrogen (Carlsbad, CA) and cycloheximide was from MP Biomedicals (Irvine, CA). Lovastatin, synthesized by Merck (Whitehouse Station, NJ) was provided by T. Y. Chang (Dartmouth Medical School, Dartmouth, NH).

This article was published online ahead of print in *MBoC in Press* (http://www.molbiolcell.org/cgi/doi/10.1091/mbc.E09–07–0605) on March 3, 2010.

Address correspondence to: Charles Barlowe (barlowe@dartmouth.edu).

Abbreviations used: COPII, coat protein complex II; DTT, dithiothreitol; PC-PLC, phosphatidylcholine phospholipase C; PI, phosphatidylinositol; PI-PLC, phosphatidylinositol phospholipase C; tER, transitional ER.

Table 1. *S. cerevisiae* strains used in this study

Strain	Genotype	Source
FY834	*Mat α his3 ura3 leu2 lys2 trp1*	Winston *et al*. (1995)
RPY18	*MAT a ura3 leu2 his3 trp1 ade8 sec24-11*	Peng *et al*. (2000)
CBY266	*Mat a leu2 ura3 trp1 lys2 ade2 sed5-1*	Barlowe strain collection
CBY267	*MAT α trp1 ade2 ura3 leu2 can1*	Cao and Barlowe (2000)
CBY302	*Mat α leu2 lys2 ura3 trp1 uso1-1*	Barlowe strain collection
CBY325	*Mat a his3 ura3 leu2 lys2 trp1 sec13-1*	Barlowe strain collection
CBY478	*Mat α his3 ura3 lys2 ypt1-3*	Barlowe strain collection
CBY545	*Mat α his3 leu2 trp1 ura3 sec18-1*	Barlowe strain collection
CBY558	*Mat α his3 leu2 trp1 ura3 sec12-4*	Barlowe strain collection
CBY595	*MAT a ura3 leu2 his3 trp1 ade8*	Peng *et al*. (2000)
CBY615	*Mat a his3 trp1 ura3 sec23-1*	Powers and Barlowe (2002)
CBY664	*Mat α leu2 ura3 his3-200 sec16-2*	Powers and Barlowe (2002)
CBY740	*MAT α his3 leu2 lys2 ura3*	Research Genetics (Huntsville, AL)
CBY1336	*Mat a ura3 leu2 yip1::KAN (pRS315 yip1-4 ts)*	Calero *et al*. (2003)
CBY1772	*CBY558, SEC13::SEC13-GFP-URA3*	This study
CBY1829	*FY834, SEC13::SEC13-GFP-URA3*	This study
CBY1860	*CBY740, SEC23::SEC23-GFP-URA3*	This study
CBY1999	*CBY664, SEC13::SEC13-GFP-URA3*	This study
CBY2013	*CBY302, SEC13::SEC13-GFP-URA3*	This study
CBY2014	*CBY545, SEC13::SEC13-GFP-URA3*	This study
CBY2015	*CBY478, SEC13::SEC13-GFP-URA3*	This study
CBY2084	*FY834, ura3-52::SEC13-GFP-URA3*	This study
CBY2085	*CBY615, ura3-52::SEC13-GFP-URA3*	This study
CBY2086	*CBY1336, ura3-52::SEC13-GFP-URA3*	This study
CBY2709	*CBY664,)SEC23::SEC23-GFP-URA3*	This study
CBY2710	*CBY558, SEC23::SEC23-GFP-URA3*	This study
CBY2711	*CBY545, SEC23::SEC23-GFP-URA3*	This study
CBY2712	*FY834, SEC23::SEC23-GFP-URA3*	This study
CBY2716	*FY834, SEC63::SEC63-RFP-HIS3MX6*	This study
CBY2717	*CBY267, SEC13::SEC13-GFP-URA3*	This study
CBY2718	*CBY267, pRS316-SEC23-GFP*	This study
CBY2719	*CBY266, pRS316-SEC23-GFP*	This study
CBY2720	*CBY478, pRS316-SEC23-GFP*	This study
CBY2744	*MAT α his3 leu2 lys2 ura3 pep4::KAN*	Research Genetics (Huntsville, AL)
CBY2835	*CBY2744, SEC23::SEC23-GFP*	This study
CBY2837	*CBY2835, Yep351-SEC23-GFP, pRS423-SEC24-HIS$_6$*	This study
CBY2969	*CBY1829, SEC63::SEC63-RFP-HIS3MX6*	This study
CBY3106	*CBY595, SEC13::SEC13-GFP*	This study
CBY3107	*CBY595, SEC23::SEC23-GFP*	This study
CBY3108	*RPY18, SEC13::SEC13-GFP*	This study
CBY3109	*RPY18, SEC23::SEC23-GFP*	This study
CBY3130	*CBY325, SEC23::SEC23-GFP*	This study

Antibodies and Immunoblotting

Antibodies against Sec13p (Salama *et al*., 1993), Sec23p (Hicke and Schekman 1989), carboxypeptidase (CPY) (Rothblatt *et al*., 1989), and anti-actin monoclonal immunoglobulin (Ig)G from Affinity BioReagents (Rockford, IL) have been described. For immunoblots, proteins were resolved on SDS-polyacrylamide gel electrophoresis, transferred to nitrocellulose, and filter bound primary antibodies were detected using the SuperSignal chemiluminescence method (Pierce Chemical, Rockford, IL) and imaged with a bioimaging system (UVP, Upland, CA).

Yeast Strains and Plasmids

S. cerevisiae strains used in this study are listed in Table 1. All yeast transformations were performed according to the standard lithium acetate transformation procedure (Ito *et al*., 1983).

The pUC19 based *SEC13-GFP* or *SEC23-GFP* integrating plasmids (Rossanese *et al*., 1999) were used to replace *SEC13* and *SEC23* sequences with *SEC13-GFP* and *SEC23-GFP*, respectively. Strains that could not tolerate Sec13p-green fluorescent protein (GFP) as a sole copy of Sec13p were transformed with an EcoRV-linearized version of pUC19 containing the *SEC13-GFP-URA3* sequence. This plasmid integrated at the *URA3* chromosomal locus of *ura3-52* strains. To create the plasmid, a region of the *SEC13* open reading frame was amplified by polymerase chain reaction (PCR) from genomic DNA and digested with KpnI and BstEII. This PCR product was ligated into *pUC19-SEC13-GFP* digested with the same enzymes. Strains that could not tolerate Sec23p-GFP as a sole copy of Sec23p were transformed with pRS316-SEC23-GFP. This plasmid was created by subcloning the carboxy-terminus of SEC23-enhanced green fluorescent protein (GFP) sequence from *pUC19-SEC23-GFP* into the multiple cloning site of pRS316 by using EcoRI and HindIII. The N-terminal region of the *SEC23* open reading frame was then subcloned from pTYY121 (Barlowe *et al*., 1994) by using SacI and BspEI, resulting in pRS316-SEC23-EGFP.

The plasmid containing the *RFP-HIS3MX6* sequence within a Longtine cassette has been described previously (Scarcelli *et al*., 2007). *SEC63* was replaced in the indicated strains with *SEC63-RFP-HIS3MX6* as described previously (Longtine *et al*., 1998).

Growth Conditions and Media

Yeast strains were grown in YPD medium (1% Bacto-yeast extract, 2% Bacto-peptone, and 2% dextrose) unless indicated otherwise. Temperature-sensitive strains were grown at 20°C (permissive temperature) to mid-log phase and shifted to 37°C (restrictive temperature), as indicated. Synthetic complete medium used for the selection of transformants and cerulenin treatment was from Bio 101 (Vista, CA). Synthetic complete medium for inositol starvation was prepared as described previously (Jesch *et al*., 2005), with or without 75 μM inositol.

For inhibition of protein synthesis with cycloheximide, cell cultures were grown to early log phase at 20°C, cultures were divided in two, and one half received 0.1 mg/ml cycloheximide. All cultures were then incubated at 20°C for 30 min, and then cells were imaged. Cultures were then transferred to 37°C, and then cells were imaged after 10, 30, 60, and 120 min. To ensure that protein translation was inhibited, wild-type cells (CBY1829) were treated with 0.1 mg/ml cycloheximide in parallel, and samples (5 OD_{600} units) collected

after 0, 15, and 60 min of treatment for analysis of cell lysates by immunoblot (Otte *et al*., 2001).

For induction of unfolded protein response with dithiothreitol (DTT), wild-type cells (CBY1829) were grown to early log phase and the culture divided in two. One half received 8 mM DTT, and cells were removed from cultures after 15, 30, 60, and 120 min for imaging. In a separate experiment, wild-type cells (CBY1829) were treated with DTT; samples collected after 0, 15, and 60 min; and lysates analyzed by immunoblot as described above.

For inhibition of fatty acid synthesis with cerulenin, cells were grown in synthetic complete medium at 30°C to early log phase. The cultures were split in two, and one half received 20 μg/ml cerulenin from a 20 mg/ml ethanolic stock. The other half received an equal volume of ethanol as control. Cell samples were removed from the cultures after 1, 2, and 3 h for image analysis. Wild-type cells (CBY1829) were monitored in a pulse-chase experiments after cerulenin treatment. Cells were grown in synthetic complete medium to an OD_{600} of ~0.5 and 20 μg/ml cerulenin was added to the test culture; a corresponding amount of ethanol was added to the control culture. After 2 h of treatment, pulse-chase analysis to monitor CPY maturation was performed as described previously (Belden and Barlowe, 1996).

Microscopy

Still images were acquired using an BX51 microscope (Olympus, Tokyo, Japan) equipped with a 100-W mercury arc lamp, Plan Apochromat 60× objective (1.4 numerical aperture), and a Sensicam QE charge-coupled device camera (Cooke, Romulus, MI) powered by IPLab software (BD Biosciences, San Jose, CA). The microscope was equipped with an Endow GFP BP filter set (Chroma Technology, Brattleboro, VT) for GFP fusion protein visualization, an XF06 filter set (Omega Optical, Brattleboro, VT) for 4,6-diamidino-2-phenylindole (DAPI) visualization, and an HQ:TRITC (Rhodamine)/Di I filter set (Chroma Technology) for red fluorescent protein (RFP) fusion protein visualization. The 30-s videos were acquired using a Zeiss Axioplan 2 microscope (Carl Zeiss, Thornwood, NY), equipped with an Orca II cooled charged-coupled device camera (Hamamatsu, Bridgewater, NJ) and OpenLab software (Improvision, Lexington, MA).

The 4-min video was acquired on an UltraVIEW VoX spinning disk confocal imaging system (PerkinElmer Life and Analytical Sciences, Boston, MA), mounted upon a TE-2000 microscope (Nikon, Tokyo, Japan). The laser excitation wavelength of 488 nm was used at 62% of laser power, and one image per second was acquired. For fluorescence recovery after photobleaching (FRAP) experiments, the same system and laser beam were used to photobleach Sec13p-GFP–positive puncta to 60% of the initial fluorescence intensity of the puncta. Recovery of the GFP signal was monitored by acquiring four z-series images within a 1-μm section of the cells, every 0.4 s. The z-series images were used to create a maximal intensity projection image for each time point. A region of interest was selected around the bleached puncta to determine signal intensity with Velocity software (Velocity Software, Mountain View, CA). Mean intensities of the region of interest were used to determine signal recovery time.

For live cell imaging, cells expressing Sec13p-GFP or Sec23p-GFP fusion proteins were grown to mid-log phase. A portion (500 μl) of the cultures was harvested, and cell pellets resuspended in 20 μl of water. Two to 3 μl of resuspended cells was placed on the slide and viewed immediately.

Image Analysis

In all figures, the scale bar indicates a length of 5 μm. Still images were analyzed using IPLab software. To determine fluorescence intensity per puncta, a circular region of interest (ROI) with an area of 32 pixels was used to determine the total fluorescence of each individual puncta within 10 cells. Background was determined by placing the ROI outside of cells and averaging six different ROI readings per image. Fluorescence values were adjusted by subtracting background fluorescence from raw readings. Individual total tER site fluorescence intensities were plotted for different strains and growth temperatures, as indicated. The fraction of live cell populations showing altered tER site morphologies resulting from temperature shift or drug treatment was determined manually by analyzing 40–100 cells per condition.

For analysis of in vitro tER site reconstitution images, total fluorescence intensity per semi-intact cell was determined in a similar way, using a larger ROI to surround each semi-intact cell completely. Only the cells that seemed perforated were chosen for this analysis, characterized by their "convoluted" appearance on differential interference contrast (DIC) images, and their permeability to the DAPI stain. Analyses of five to 30 semi-intact cells were background subtracted, and the average total fluorescence intensities per condition or time point were determined, as indicated above.

Production of Sec23p-GFP–containing Cytosol for In Vitro Budding and tER Site Assembly Assays

CBY1860 cells (3 liters) were grown in YPD to OD_{600} of 1.2–1.5, yielding ~15 g of cells. Cells were washed in buffer 88 (20 mM HEPES, pH 7.5, 250 mM sorbitol, 150 mM KOAc, and 5 mM MgOAc) and resuspended in 2 ml of buffer 88 supplemented with 1 mM DTT and 1 mM phenylmethylsulfonyl fluoride (PMSF). Cells were lysed by a bead-beat method (Rexach and Schekman, 1991), and unlysed cells were cleared by low-speed centrifugation. The cell lysate was further clarified by centrifugation at 30,000 × *g* for 15 min and then 175,000 × *g* for 15 min. Cytosols were stored at −70°C.

In Vitro COPII-dependent Vesicle Budding

COPII-dependent budding reactions were performed using semi-intact cell membranes containing [^{35}S]glyco-pro-α-factor translocated into the ER as described previously (Baker *et al*., 1988; Rexach *et al*., 1991). Budding reactions were supplemented with membranes, ATP regeneration system, guanosine triphosphate (GTP), and ~80 μg of Sec23p-GFP–containing cytosol (Baker *et al*., 1988; Barlowe, 1997). For preparation of *sec12-4* membranes, cultures were grown at 20°C and converted to semi-intact cells (Rexach *et al*., 1991). For reactions containing PC-PLC or PI-PLC, semi-intact cell membranes were mixed with the indicated amounts of lipase in a total volume of 7 μl and incubated at 4°C for 10 min, before the addition of the remaining components. To assess ER membrane integrity after incubation with indicated lipases, protease protected [^{35}S]glyco-pro-α-factor was measured after treatment of membrane with trypsin for 10 min followed by trypsin inhibitor as described previously (Rexach and Schekman, 1991).

Reactions that assayed the budding potential of semi-intact cells that were starved for inositol contained purified COPII proteins (Barlowe, 1997) and as indicated, reactions were supplemented with 50 μg of unfractionated cytosol (CBY740) or with 12 μl of fractions from the Superose 6 column (GE Healthcare, Little Chalfont, Buckinghamshire, United Kingdom) elution profile.

In Vitro Reconstitution of tER Sites

All procedures before imaging were performed at 4°C. Reactions (25 μl) were assembled as in COPII-dependent budding reactions, by using previously described amounts of semi-intact cell membranes but no [^{35}S]pre-pro-α-factor (Baker *et al*., 1988; Barlowe, 1997). Reactions were supplemented with 80 μg of Sec23p-GFP–containing cytosol and Sar1p or Sar1p T37N was added (2 μg/ml) where indicated. Reactions were incubated at 4°C for 30 min, supplemented with DAPI, and a 2- to 3-μl aliquot of reactions was placed on a slide and imaged immediately. For time course experiments, images were captured from the same slide over a 10-min period at 23°C. Where indicated, GTP was replaced with 100 μM guanosine 5′-*O*-(3-thio)triphosphate (GTPγS). PC-PLC and PI-PLC treatments were as described above. To reconstitute Sec23-GFP assembly at tER sites with purified proteins, previously described amounts of Sar1p and Sec13p/31p (Barlowe, 1997) were supplemented with 2 μg/ml purified Sec23p–GFP/Sec24p complex.

Expression and Purification of Sar1 T37N

The T37N mutation was generated by the QuikChange site-directed mutagenesis kit (Stratagene, La Jolla. CA) in the *SAR1-GST* sequence in plasmid pTY40 (Barlowe *et al*., 1994), according to the manufacturer's instructions. The resulting plasmid was used to express Sar1(T37N)-GST in *Escherichia coli* strain BL 21, and protein was purified as described previously (Barlowe *et al*., 1994).

Expression and Purification of the Sec23p-GFP/Sec24p Complex

To express Sec23-GFP from a multicopy vector, the HindIII fragment of pTYY121 (Barlowe *et al*., 1994), which contains the *SEC23* open reading frame was replaced with the HindIII fragment of pRS316-SEC23-GFP (this study), resulting in plasmid YEp351-SEC23-GFP. For *SEC24* expression, the ~3850-base pair region of pTYY117 containing SEC24-HIS_6 was amplified by PCR using primer 1 (CGACTAGAGC TCGGAGAGTC AAACTGTAAA GGCGAATC), with a SacI restriction site; and primer 2 (CGATAGCTCG AGTTAGTGAT GGTGATGATG ATGTTTGCTA ATTCTGGCTT CATGAT) containing a HIS_6 tag, stop codon, and XhoI site. The PCR product was blunted and ligated into pGEM-T Easy vector (Promega, Madison, WI), according to the manufacturer's instructions. The ligation product was digested with SacI and XhoI, and the fragment containing the *SEC24-HIS*$_6$ sequence was ligated into the SacI-XhoI fragment of pRS423. The resulting plasmids, YEp351-SEC23-GFP and pRS423-SEC24-HIS_6, were transferred into CBY2835, which contained SEC23-GFP at the chromosomal *SEC23* locus, to yield CBY2837.

A 15-liter culture of CBY2837 cells was grown in synthetic medium lacking leucine, uracil, and histidine to an OD_{600} of ~1.0. Cells were harvested and Sec23p–GFP/Sec24p complex purified as described previously (Barlowe *et al*., 1994). Aliquots of the protein were stored at −70°C.

Fractionation of Yeast Cytosol by Superose 6 Chromatography

CBY740 cells were grown in 9 l of YPD at 30°C to OD_{600} of ~1.4. Harvested cells were used to prepare a liquid nitrogen-lysed cytosol (Barlowe *et al*., 1994), with minor modifications. A 50-g cell pellet was resuspended in a final volume of 22 ml of buffer 88, containing 1 mM DTT and 1 mM PMSF. The medium-speed supernatant fraction was centrifuged at 89,000 × *g* for 60 min. The resulting supernatant was diluted with 0.2 volumes of buffer 88 containing 1 mM DTT and 1 mM PMSF and centrifuged at 175,000 × *g* for 15 min. The supernatant yielded ~10 mg/ml protein and was stored at −70°C. A

fraction of this supernatant (0.5 ml) was loaded on a Superose 6 column (GE Healthcare) equilibrated in running buffer (20 mM HEPES, pH 7.5, 150 mM KOAc, and 5 mM MgOAc), and developed with 3 column volumes of running buffer at 0.3 ml/min. Elution fractions (2 ml) were collected and stored at −70°C.

RESULTS

Sec13p-GFP and Sec23p-GFP Localize to tER Sites in S. cerevisiae

COPII subunits localize to stable tER site domains in animal cells, invertebrates, and the yeast *Pichia pastoris* (reviewed by Kirk and Ward, 2007). However, in the yeast *S. cerevisiae*, fluorescence microscopy of Sec13p-GFP and Sec23p-GFP documented numerous smaller puncta that seemed evenly distributed throughout the cytoplasm (Rossanese *et al*., 1999). The behavior of these smaller COPII structures has not been extensively studied, and it was thought that individual puncta could simply represent individual vesicles emerging from ER membranes. We sought to characterize the properties of these COPII structures in *S. cerevisiae* to determine whether studies on this model system could contribute to our understanding of tER structure and function.

To visualize COPII puncta in *S. cerevisiae*, *SEC13-GFP* or *SEC23-GFP* were integrated into the *SEC13* or *SEC23* loci, respectively, by gene replacement. Puncta were observed in wild-type cells expressing Sec13p-GFP or Sec23p-GFP by fluorescence microscopy, obtaining live cell images in a single focal plain. Sec13p-GFP and Sec23p-GFP localized to 15–25 distinct spots per cell in the perinuclear region and also distributed around the cell periphery (Figure 1A). Initial inspection indicated that individual COPII marked structures persisted for several seconds, when monitored by conventional fluorescence microscopy. Over longer exposure times (10–15 s), the puncta seemed relatively stable and localized to areas of the *S. cerevisiae* ER.

On further inspection, several lines of evidence indicated that Sec13p-GFP and Sec23p-GFP localized to tER site structures in *S. cerevisiae*, rather than marking individual coated vesicles. Images captured after longer exposure times in a single focal plane near the center of the cell revealed that the puncta were not evenly distributed throughout the cytoplasm but that their localization was restricted to areas that coincided with ER membranes (Figure 1A). To confirm colocalization of Sec13p-GFP puncta with the ER, Sec63-RFP was coexpressed in wild-type cells. Images taken in both GFP and RFP channels indicated that Sec13p-GFP puncta are contiguous with Sec63-RFP marked ER (Figure 1B).

The motion and stability of COPII marked puncta were investigated using real-time imaging microscopy. We detected random movement of these structures by fluorescence microscopy (Supplemental Video 1). Motion was restricted to the perinuclear region or the cell periphery, consistent with tER site localization. To minimize photobleaching and extend signal detection time, tER site dynamics were investigated by spinning disk confocal microscopy (Figure 1C and Supplemental Video 2). Time course imaging was extended up to 4 min, and 1 image per 0.4 s was captured to enable us to follow the location of individual spots. Some puncta disappeared early in the time course, perhaps due to movement out of the focal plane. In other areas, puncta disappeared and returned several times during the experiment. It was not technically feasible to monitor all puncta throughout this extended time course. However, several of the brighter puncta were tracked in the same focal plane over several images and persisted during the entire 239 s (Figure 1C, arrowheads). The longevity and movement of such puncta were more consistent with the behavior of tER sites, rather than transport vesicles. Previous reports indicate that the half-life of secretory protein delivery from the ER to the Golgi complex is ~1 min (Losev *et al*., 2006). Therefore, if Sec13p-GFP marked puncta were coated vesicles, we would expect most of these transport intermediates to uncoat and fuse with the Golgi apparatus in under a minute. Instead, the persistence of these sites for up to 4 min is more consistent with a type of stabilized tER domain on the ER surface.

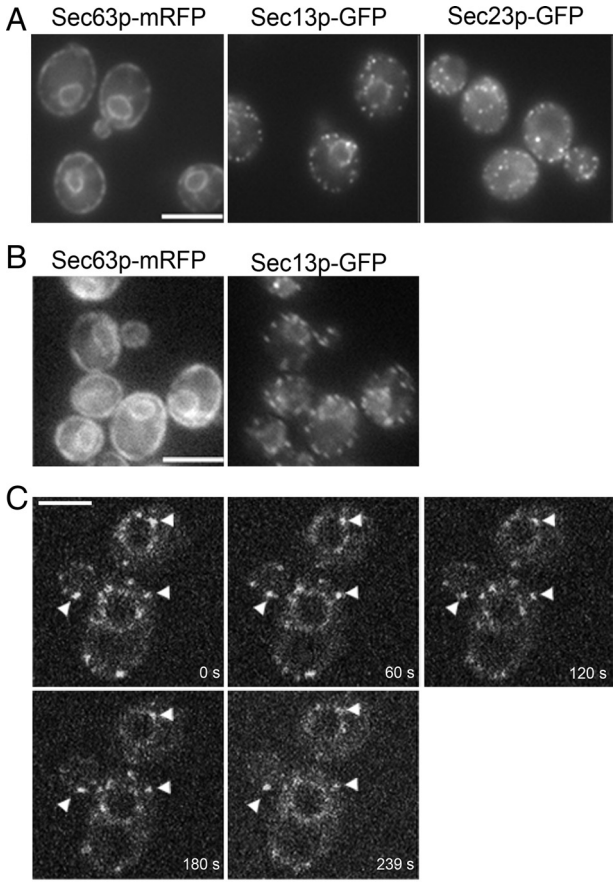

Figure 1. Live cell microscopy shows that Sec13p-GFP and Sec23p-GFP localize to tER sites on the ER membrane. (A) Still images of wild-type strains expressing Sec63-mRFP (CBY2716), Sec13p-GFP (CBY1829), and Sec23p-GFP (CBY2712). Note that both Sec13p-GFP and Sec23p-GFP punctae localize to the ER vicinity, outlined in the cell periphery and perinuclear region by Sec63p-mRFP. (B) A wild-type strain (CBY2969), expressing both Sec13p-GFP and Sec23p-GFP, was imaged in the GFP and the RFP channels. Note significant overlap between ER and Sec13p-GFP punctae. (C) Still images from a video of cells expressing Sec13p-GFP (CBY1829), acquired by four-dimensional spinning disk confocal microscopy. Numbers indicate the time in seconds from start of acquisition. Arrowheads indicate the position of tER sites that could be tracked through each of the video frames. Bars, 5 μm.

In addition, the turnover kinetics of Sec13p-GFP was analyzed in a photobleaching experiment (Supplemental Figure S1). Sec13p-GFP intensity at several tER sites was reduced with a 488 nm laser beam, and fluorescence recovery time was monitored by spinning disk confocal microscopy. The half-time of recovery was estimated as ~3 s, which is similar to that reported for Sec23p-GFP in animal cells (Forster *et al*., 2006) and suggests analogous behavior of COPII coat subunits at tER sites in *S. cerevisiae*. Further studies on the turnover rates for each COPII subunit under varying

Table 2. Summary of tER morphologies observed in temperature-sensitive mutants

Function	Mutation	Sec13p-GFP distribution	Sec23p-GFP distribution
Vesicle budding	*sec12-4*	Large puncta[a]	Large puncta
	sec16-2	Large puncta	Large puncta
	sec23-1	Altered[b]	nd
	sec24-11	wt	Altered
	sec13-1	nd	Altered
	sec31-1	wt	wt
	yip1-4	wt	wt
Vesicle fusion	*uso1-1*	wt	wt
	sed5-1	wt	wt
	sec18-1	wt	wt
	ypt1-3	wt	nd

nd, not determined; wt, wild type.

[a] Large puncta, >50% of cells accumulate one to two large bright puncta.

[b] Altered, >50% of cells display one to two brighter puncta and/or a diffuse GFP pattern.

conditions will be necessary to fully characterize coat dynamics. However, based on our collective findings we conclude that COPII-marked puncta in *S. cerevisiae* represent tER site structures that are smaller but share similar properties with tER sites described in other species.

Conditional Mutations That Inhibit COPII Vesicle Budding, but Not Tethering or Fusion, Affect tER Site Morphology

ER–Golgi transport in yeast includes the stages of COPII-coated vesicle budding from the ER, followed by vesicle tethering and fusion of vesicles with Golgi membranes. Temperature-sensitive mutants impaired in each of the transport stages exhibit ER membrane expansion and a block in cargo secretion at restrictive temperatures. In vesicle-budding mutants, ER membranes accumulate due to an arrest in vesicle production (Novick *et al*., 1980; Kaiser and Schekman, 1990). In vesicle-tethering and fusion mutants, budded vesicles accumulate and Golgi membrane structures are diminished (Kaiser and Schekman, 1990; Nakajima *et al*., 1991; Morin-Ganet *et al*., 2000). In addition, inhibition of membrane fusion is thought to ultimately prevent recycling of vesicle components back to the ER and to inhibit production of new ER-derived vesicles, thus causing an accumulation of ER membranes (Novick *et al*., 1980; Lewis and Pelham, 1996; Wooding and Pelham, 1998).

We examined tER site morphology in a set of temperature-sensitive strains bearing mutations in genes that are essential for vesicle budding, tethering, or fusion. The tER site markers Sec13p-GFP and Sec23p-GFP were expressed in these mutant strains and their distributions were compared with wild-type strains at 20°C (permissive temperature) and 37°C (restrictive temperature). Liquid cultures were grown to mid-log phase at permissive temperature and then shifted to the restrictive temperature, with images collected over a 120-min time course (Table 2 and Figure 2).

Figure 2 shows tER site morphologies that were observed in vesicle budding and fusion mutants, compared with wild type. At a permissive temperature (20°C), wild-type and mutant cells showed similar tER site brightness and distribution. However, *sec12-4* (budding mutant) cells exhibited altered tER site morphology within minutes after the shift to restrictive temperature. tER sites in wild type and *uso1-1* cells (tethering mutant) remained unchanged within this time frame (Figure 2A). A fraction of the *sec12-4* cell population began to accumulate large bright puncta 4 min after the temperature shift, as determined by time lapse imaging (data not shown). By 15 min at the restrictive temperature, 50% of *sec12-4* cells exhibited this altered tER site morphology, and >90% of the cells did so after 2 h (Figure 2C). Quantification of total fluorescence intensity per puncta in

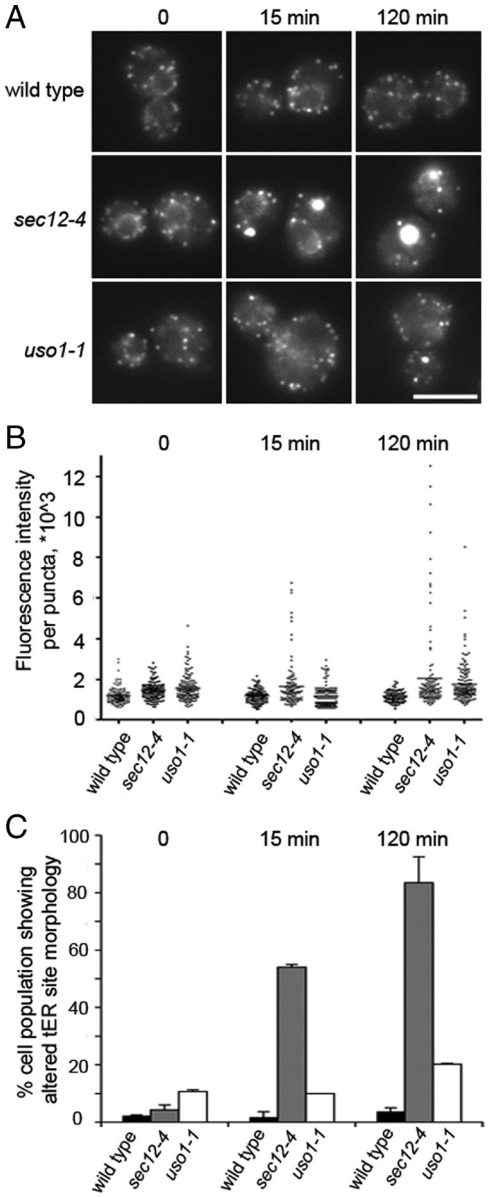

Figure 2. Vesicle-budding mutant *sec12-4* cells, but not wild-type or fusion mutant *uso1-1* cells, exhibit altered tER site morphology at a restrictive temperature. (A) Wild-type (CBY1829), *sec12-4* (CBY1772) and *uso1-1* (CBY2013) strains were grown at 22°C, imaged, and then shifted to 37°C. Images were acquired at 0, 15, and 120 min after the shift. (B) Quantification of total fluorescence intensities of individual tER sites from the images obtained in A. All tER sites were analyzed in 10 randomly selected cells per condition. Points on the plot indicate individual fluorescence intensity values. (C) Quantification of the percentage of cell populations that showed altered tER site morphology, from the images obtained in A. Forty randomly selected cells were analyzed per condition.

10 randomly chosen cells confirmed that *sec12-4* cells acquired one to three very bright puncta at 37°C (Figure 2B). Brightness of these atypical puncta in *sec12-4* cells peaked after 2 h at restrictive temperature. Moreover, the *sec12-4* block reduced the total number of puncta, suggesting that individual tER sites fuse or aggregate into the larger structures while COPII proteins remain bound. Interestingly, *sec12-4* cells did retain a reduced population of tER sites with normal brightness, suggesting that not all tER sites are identical. Only a small number of the *uso1-1* cells displayed slightly brighter puncta after 2 h at restrictive temperature, but the brightness of these structures remained lower than that of the *sec12-4* puncta (Figure 2, B and C). Controls showed that fluorescence intensity of individual tER sites in wild-type cells remained relatively constant throughout the shift to 37°C. The images shown follow Sec13p-GFP, although Sec23p-GFP puncta were altered in a similar way in *sec12-4* cells and similarly unaffected in wild type or *uso1-1* cells (data not shown).

The conditional vesicle-budding mutant *sec16-2* also showed an accumulation of large bright puncta when shifted to the restrictive temperature, similar to *sec12-4* cells. In contrast, the vesicle-budding mutants *sec23-1* and *sec13-1* displayed altered tER site morphologies with an accumulation of intermediate-sized GFP marked puncta (Supplemental Figure S2 and results summarized in Table 2). The *sec24-11* mutant also accumulated intermediate sized puncta when Sec23p-GFP was monitored but not with Sec13p-GFP, perhaps due to a synthetic effect of the GFP fusion on mutant Sec23/24 complex. Interestingly, GFP marked tER sites retained a wild-type appearance in the *sec31-1* and *yip1-4*–budding mutants at a restrictive temperature after cell growth was clearly abolished (Table 2). In addition, observation of Sec13p-GFP or Sec23p-GFP in the postbudding *uso1-1*, *ypt1-3*, *sec18-1*, and *sed5-1* mutants indicated little or no change in tER site morphology at restrictive temperatures (Table 2).

In summary, we observed that general inhibition of ER export, and the expansion of ER membranes that accompany such blocks, were not sufficient to alter tER site morphology. However, many of the mutations that directly act early in assembly of the COPII vesicle coat exhibited dramatic changes in Sec13-GFP and Sec23-GFP distribution. The lack of change in the *yip1-4* mutant, which is thought to inhibit vesicle budding after coat assembly (Heidtman *et al.*, 2003), suggests that a block in budding per se is not sufficient to perturb tER site structure.

Cycloheximide Treatment Partially Preserved Wild-Type tER Site Appearance in sec12-4 and sec16-2 Cells

Several studies have shown colocalization of COPII coat proteins with secretory cargo at ER exit sites in mammalian cells (Kirk and Ward, 2007). We hypothesized that cargo accumulation may contribute to generation of the large bright COPII puncta that appear in vesicle-budding mutants, such as *sec12-4*. To test this hypothesis, protein synthesis was inhibited with cycloheximide, and tER site structure was then observed after shifting cells to a restrictive temperature. Wild-type cells treated with cycloheximide for 15 and 60 min are depleted of secretory cargo in the ER, such as procarboxypeptidase Y (pro-CPY), confirming effective inhibition of translation (Figure 3A). Under this condition, wild-type cells expressing Sec13p-GFP did not display altered tER site morphologies (data not shown). However, cycloheximide treatment of the *sec12-4* and *sec16-2* strains for 30 min at 20°C before shift to 37°C influenced tER site morphologies in these mutants (Figure 3B). A significantly

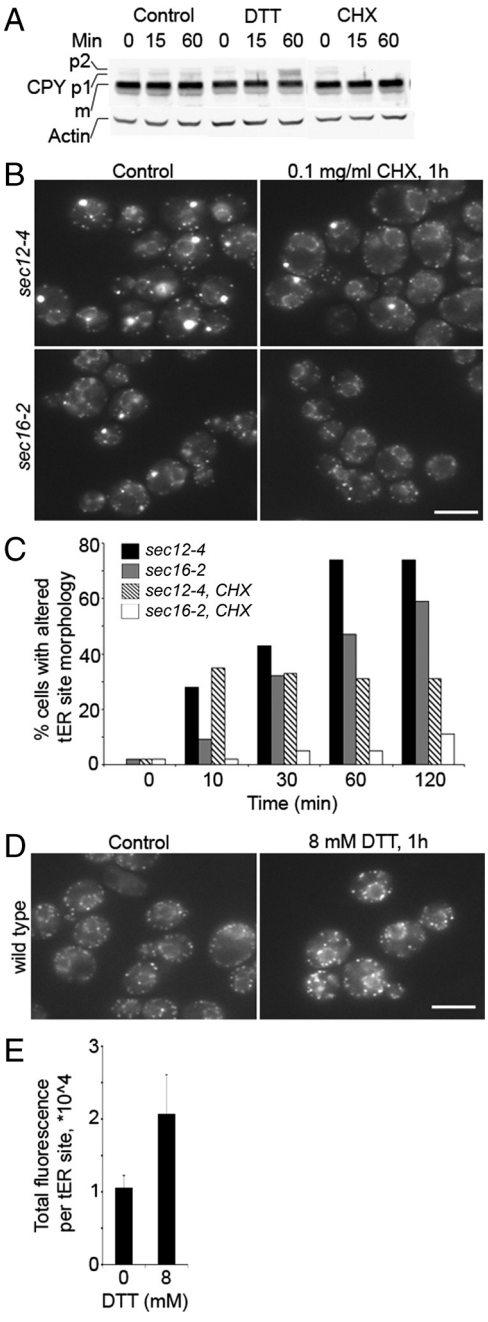

Figure 3. Influence of secretory cargo on tER site morphology. (A) Wild-type cells expressing Sec13p-GFP (CBY1829) were treated with 8 mM DTT or 0.1 mg/ml cycloheximide for indicated times. Cells were collected and whole cell lysates assessed for CPY and actin (loading control) by immunoblot. Note accumulation of p1 CPY (ER form) in DTT-treated cells and depletion of p1 CPY in cycloheximide-treated cells compared with wild type. (B) *sec12-4* (CBY1772) and *sec16-2* (CBY1999) cells expressing Sec13p-GFP were grown at 20°C, treated with 0.1 mg/ml cycloheximide for 30 min, and then shifted to 37°C. Cells were imaged at 0-, 10-, 30-, and 60-min time points after temperature shift, and images are shown at the 30-min time point (1 h after receiving cycloheximide). (C) Quantification showing the percentage of cells with altered tER site morphology from experiment shown in B. At least 150 cells were counted per condition. (D) Wild-type cells expressing Sec13p-GFP (CBY1829) were grown to mid-logarithmic phase, treated with 8 mM DTT, and imaged after 1 h. (E) Total fluorescence intensity per tER site was analyzed in 10 randomly selected cells per condition, from the images shown in D.

greater proportion of mutant cells treated with cycloheximide exhibited a wild-type tER site distribution at the restrictive temperature (60–70% of the population), compared with untreated cells (10–30% of cells; Figure 3C). Therefore, inhibition of protein synthesis partially preserved the wild-type tER site appearance in *sec12-4* and *sec16-2* mutants. These observations suggest that the observed collapse of tER structures into larger COPII aggregates in early budding mutants may be induced through an accumulation of nascent secretory cargo at aborted vesicle formation sites.

Previous studies indicated that activation of the unfolded protein response was required in animal cells to increase tER site number and intensity upon overexpression of secretory cargo for 24 h (Farhan *et al*., 2008). We observed in yeast that activation of the unfolded protein response by treatment of cells with 8 mM DTT increased the total fluorescence per tER site by approximately twofold (Figure 3, D and E). However, significant changes in tER site number or Sec13p-GFP expression level were not detected after the 2-h DTT treatment (data not shown). Accumulation of unfolded cargo at tER sites may decrease the off-rate of COPII coat subunits from the vesicle-budding sites, resulting in the apparent increased intensity. We note that accumulation of unfolded secretory proteins after DTT treatment was not sufficient to induce tER site collapse or nucleation of new tER sites. These results are consistent with the idea that both cargo accumulation and defective COPII coat assembly are necessary for generation of abnormally large tER puncta.

Inhibition of De Novo Fatty Acid Synthesis by Cerulenin Alters tER Site Morphology and Blocks Vesicle Budding from the ER

Previous reports have suggested direct involvement of membrane lipids in anterograde ER–Golgi transport. Cholesterol and ceramide levels have been reported to influence ER export and tER site properties (Sütterlin *et al*., 1997; Runz *et al*., 2006; Vacaru *et al*., 2009), whereas phosphatidylinositol 4′-monophosphate [PI(4)P] has been proposed to act in ER exit site formation in animal cells (Blumental-Perry *et al*., 2006). We analyzed lipid requirements in tER site structure and function by monitoring Sec13p-GFP and/or Sec23p-GFP localization patterns in cells containing deletions or conditional mutations at various steps of ergosterol and ceramide biosynthesis. However, no differences in tER site morphology were observed (Supplemental Table S1). tER sites also remained unaffected when ergosterol synthesis was inhibited with lovastatin or when ceramide production was inhibited with fumonisin B (Supplemental Figure S3). Both drugs were used at levels sufficient to inhibit cell growth, and images were obtained at time points where cellular integrity was maintained.

To further investigate lipid requirements for the maintenance of tER sites, we tested whether or not a more general inhibition of de novo fatty acid synthesis influenced tER site morphology. Cerulenin specifically inhibits the fatty acid synthase enzyme required for de novo synthesis of fatty acids and sterols in *S. cerevisiae* at 10–25 μg/ml (Nomura *et al*., 1972; Inokoshi *et al*., 1994; Gaspar *et al*., 2006). Because lovastatin inhibition of sterol synthesis did not disrupt tER site formation, cerulenin treatment addressed the requirement for continuous fatty acid biosynthesis in tER site maintenance.

Wild-type cells expressing Sec13p-GFP or Sec23p-GFP were grown to mid-log phase in minimal medium and treated with 20 μg/ml cerulenin. Cells were imaged at different times up to 3 h after treatment. In treated cells, Sec13p-GFP was redistributed and showed enlarged puncta around the perinuclear region (Figure 4A). Sec23p-GFP distribution was also shifted to enlarged puncta although localization to perinuclear regions was not as apparent. These changes were detected in up to 50% of the cell population after 2 h of treatment, and the number of affected cells increased after longer periods of treatment (Figure 4B). A pulse-chase experiment was performed to assess transport efficiency of the secretory protein CPY in the presence of cerulenin. Wild-type cells were treated with cerulenin for 2 h before the pulse, and the rate of CPY maturation was then monitored (Figure 4C). After a 20-min chase period, CPY was efficiently converted to the mature form in untreated cells but remained in the proform in cerulenin-treated cells. These results indicated that secretory protein transport between the ER and Golgi was blocked by cerulenin. We note that treated cells remained metabolically active and translated pro-CPY at wild-type rates after the 2-h incubation with cerulenin. Therefore, the observed influences of fatty acid synthase inhibition seem relatively specific on the secretory pathway. Moreover, addition of cycloheximide before cerulenin treatment prevented formation of the enlarged puncta (Supplemental Figure S4) as was observed for

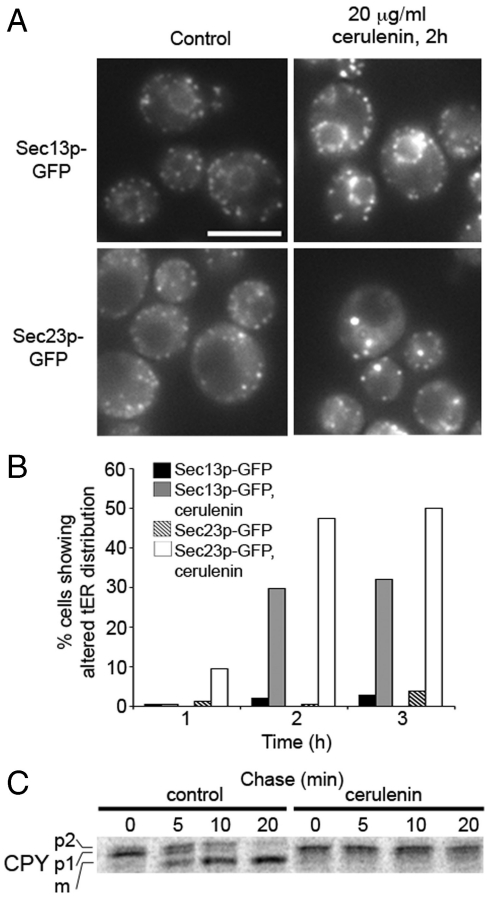

Figure 4. Cerulenin induces changes in tER site morphology and blocks CPY transport from the ER. (A) Wild-type cells expressing Sec13p-GFP (CBY1829) and Sec23p-GFP (CBY2712) were treated with 20 μg/ml cerulenin. (B) Quantification depicting the percentage of cells showing a change in tER site morphology at 1, 2, and 3 h after addition of cerulenin. At least 50 cells were analyzed per condition. (C) Pulse-chase analysis of wild-type cells (CBY740) treated with cerulenin for 2 h. Note that p1 CPY (ER form) was completely converted to the mature form (m) after 20 min of chase in control cells but accumulated in cerulenin-treated cells.

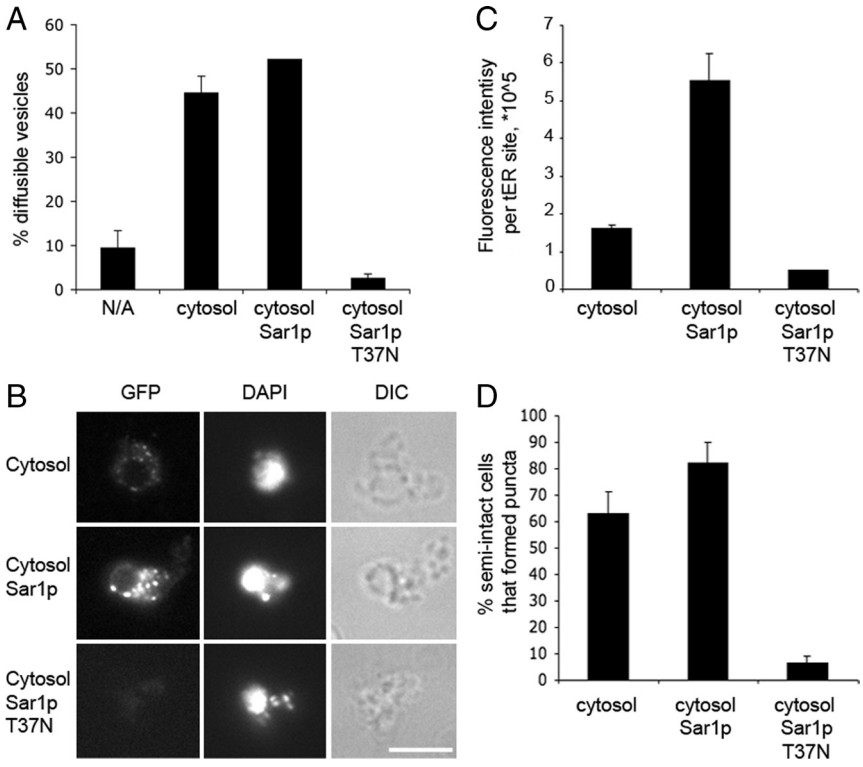

Figure 5. Reconstitution of tER site assembly in vitro from semi-intact cell membranes and cytosol. (A) Budding from washed semi-intact membranes (CBY740) containing translocated [^{35}S]gpαf after incubation at 23°C with a Sec23-GFP cytosol (CBY1860) as described under *Materials and Methods*. Reactions were supplemented with wild-type Sar1p or Sar1p T37N as indicated. Cytosol was replaced with buffer 88 in the "no addition" reaction (N/A). (B) Washed semi-intact membranes (CBY740) were incubated at 4°C with the same components as in A. After 30 min, DAPI was added and the reactions were imaged in the DIC, DAPI, and GFP channels. Note that the efficiency of Sec23p-GFP assembly into puncta and signal intensity correlate with COPII-dependent vesicle budding in A. (C) Average total cell fluorescence per reaction condition was determined from the images in B. (D) Percentage of semi-intact cells that formed fluorescent puncta was quantified from the images in B. Approximately 40 cells were analyzed per condition in C and D.

the *sec12-4* and *sec16-2* mutants. These collective findings indicate that tER site structure and function depend on continuous synthesis of fatty acids, whereas inhibition of ergosterol or ceramide production did not produce detectable effects.

Reconstitution of tER Site Assembly In Vitro with Washed Semi-Intact Cells and Sec23p-GFP–containing Cytosol

To investigate protein and lipid requirements for tER site function more directly, we established a cell free tER site assembly assay in yeast. COPII vesicle budding has been reconstituted from washed semi-intact yeast cells in vitro in the presence of cytosol or purified coat proteins (Baker *et al*., 1988; Salama *et al*., 1993). To reconstitute COPII coat recruitment to tER sites in vitro, we started with gently washed semi-intact yeast cells and supplied a cytosol containing Sec23p-GFP under conditions that recapitulate COPII-dependent budding. Temperatures between 20 and 30°C support efficient vesicle budding, whereas budding is inefficient at 4°C (Baker *et al*., 1988; Rexach and Schekman, 1991). Therefore, we provided the cytosolic factors necessary to support efficient COPII budding, incubated reactions at 4°C and then inspected cells for tER site structures by microscopy under these conditions, which would presumably accumulate COPII proteins at tER sites.

As seen in Figure 5, reaction conditions that support COPII vesicle budding at 23°C also induced tER site formation on semi-intact cells membranes at 4°C. Budding was minimal in the absence of cytosol at 23°C, was stimulated by the addition of a cytosol-containing Sec23p-GFP, and was further enhanced by adding purified Sar1p (Figure 5A). Addition of a GDP-locked mutant (Sar1p-T37N) to the reaction strongly inhibited budding, as expected (Kuge *et al*., 1994). In vitro recruitment of Sec23p-GFP to tER sites in washed semi-intact cell membranes at 4°C was increased in reaction conditions that supported vesicle budding (Figure 5B). Washed wild-type membranes incubated on ice with Sec23p-GFP–containing cytosol, GTP and an ATP regeneration system supported the formation of Sec23p-GFP fluorescent puncta. The observed Sec23p-GFP puncta resembled those seen in live cell microscopy. In some instances semi-intact cell ER and nuclear membranes seemed fragmented in DAPI stained images, which may result from the pelleting and resuspension steps during semi-intact cell washes. However, we note that the puncta assembled in vitro typically surrounded a perinuclear region, as observed for tER sites in vivo. Increasing Sar1p levels substantially increased the intensity of Sec23p-GFP signal per tER site, suggesting enhanced recruitment (Figure 5, B and C). Excess Sar1p also increased the number of semi-intact cells displaying Sec23p-GFP–positive puncta (Figure 5D). This effect is consistent with the fact that vesicle budding was stimulated in reactions containing cytosol and excess Sar1p, compared with cytosol alone. Addition of Sar1p-T37N, which completely inhibited vesicle production, also blocked recruitment of Sec23p-GFP to tER sites (Figure 5, B–D). When the total number of Sec23-GFP–positive puncta per semi-intact cell were quantified under each of these conditions, we observed on average ($N \geq 39$ cells) 5.8 puncta/cell with cytosol alone, 9.5 puncta/cell with added Sar1p, and 1.2 puncta/cell with added Sar1p-T39N. These results generally correlate with the data plotted in Figure 5C showing the percentage of semi-intact cells that form puncta. We interpret our results to indicate that the total number of tER sites per cell remains relatively constant but that addition of Sar1p increases the number of sites that recruit Sec23-GFP above a threshold level of detection. In summary, this cell-free tER site assembly assay seems to faithfully recapitulate stages in the COPII-dependent ER export process and provides a quantitative assessment of COPII assembly at tER sites.

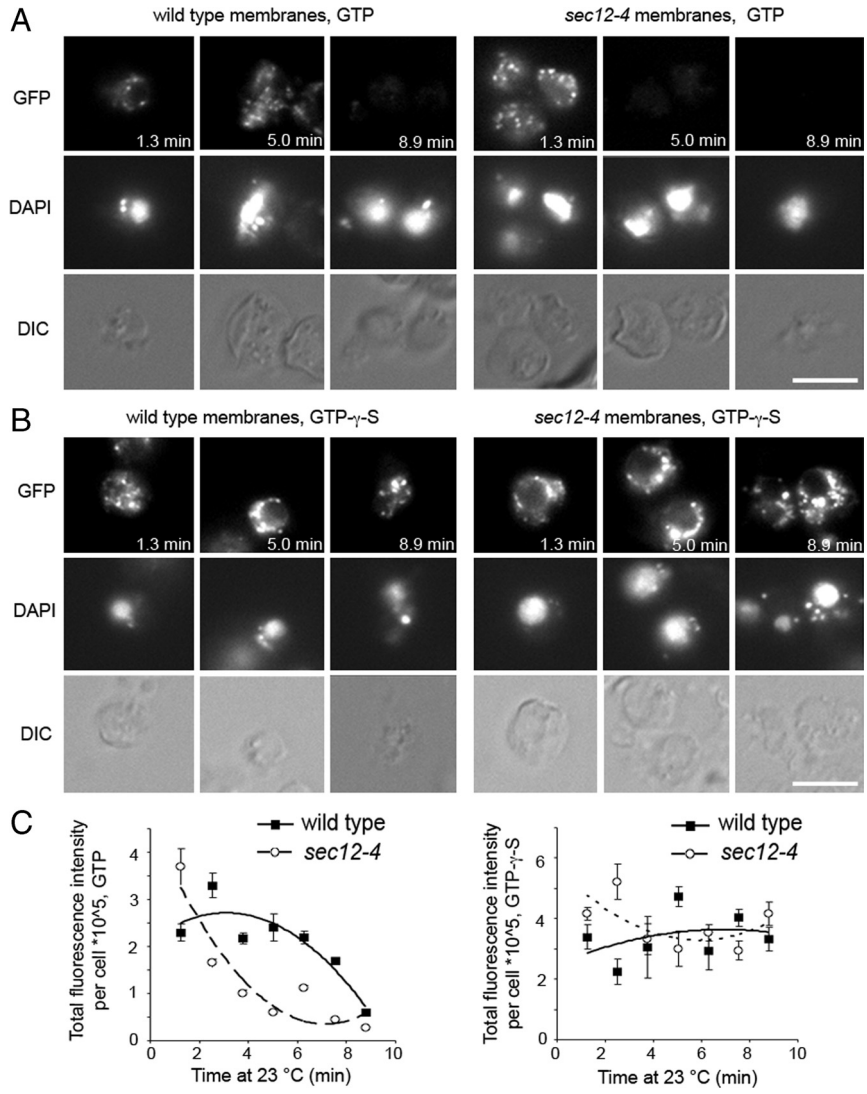

Figure 6. *sec12-4* membranes fail to recruit Sec23p-GFP to tER sites at elevated temperatures in the presence of GTP, but not GTPγS. (A) Washed wild-type (CBY80) and *sec12-4* (CBY558) semi-intact cell membranes, prepared from cultures grown at 20°C, were incubated with Sec23p-GFP cytosol (CBY1860) and Sar1p at 4°C for 30 min. DAPI was added, and a sample of each reaction was placed on a glass slide and imaged continuously at 23°C for 9 min. (B) Reactions were assembled and processed as in A, but GTP was replaced with GTPγS. (C) Plots showing total fluorescence intensity per semi-intact cell at different time points from the images obtained in A and B, analyzing five to 10 cells per time point. Note that GTPγS addition stabilizes Sec23p-GFP at tER sites in both wild-type and *sec12-4* membranes throughout the time course.

Sec23p-GFP Recruitment to tER Sites Requires the Activity of Sec12p

The in vitro measurement of Sec23p-GFP recruitment to tER sites allowed us to investigate the dynamics of coat subunit recruitment to *sec12-4* membranes. Sec12p is an essential integral membrane protein that initiates COPII coat assembly by stimulating nucleotide exchange and activation of the Sar1p GTPase (Nakano and Muramatsu, 1989; Barlowe and Schekman, 1993). Sec12p was shown to localize to tER sites in *P. pastoris* but seems dispersed in the ER membrane of *S. cerevisiae* (Nishikawa and Nakano, 1991; Nishikawa and Nakano, 1993; Rossanese *et al*., 1999) and animal cells (Weissman *et al*., 2001; Stephens, 2003). Previous studies on Sec12p suggested that mislocalization in *P. pastoris* (Soderholm *et al*., 2004) or knockdown in animal cells (Bhattacharyya and Glick, 2007) did not disrupt tER site components. Our in vivo data suggested a role for Sec12p in tER site structures, which we next investigated in vitro.

In vivo, the *sec12-4* mutation caused tER sites to collapse into larger puncta in a cargo-dependent manner (Figures 2 and 3). To explore the requirement for Sec12p activity in de novo assembly of COPII subunits at tER sites, *sec12-4* and wild-type semi-intact membranes were prepared after growth at 20°C and compared in microscopy assays that monitored Sec23p-GFP recruitment from cytosol to tER sites (Figure 6). Cell-free components were incubated on ice to induce coat recruitment and then spotted onto slides for imaging as in Figure 5. However, in these assays tER sites were monitored over a time course on the slides at 23°C. Initial time points displayed Sec23p-GFP–labeled puncta in both wild-type and *sec12-4* membranes and then, as incubations continued, the Sec23p-GFP signal at these sites was dissipated. Importantly, the rate at which Sec23p-GFP signal declined in the *sec12-4* membranes was significantly faster than in the wild-type membranes (Figure 6, A and 6C). At the 5-min time point, wild-type membranes showed intense Sec23p-GFP puncta, whereas *sec12-4* membranes no longer displayed Sec23p-GFP–positive puncta (Figure 6A). We interpret these observations to reflect an initial burst of COPII budding at tER sites in both wild-type and *sec12-4* membranes, when reactions are warmed to 23°C. In wild-type membranes, Sec23p-GFP presumably participates in several rounds of COPII vesicle budding and is recycled back to tER sites over several minutes. In *sec12-4* membranes, we propose that Sec23p-GFP participates in a limited round of COPII budding, and after the initial burst was not efficiently recruited to tER sites. A previous report indicated that *sec12-4* semi-intact cells bud vesicles after a shift to the

restrictive temperature at early time points but then budding rapidly declined (Rexach and Schekman, 1991). In this context, our results suggest that *sec12-4* semi-intact cells retained adequate levels of Sec12p activity on ice during initial Sec23p-GFP recruitment to tER sites. On vesicle budding, which was induced by sample warm-up, membrane-bound Sec23p-GFP probably exits tER sites with coated vesicles. At 23°C this mutant version of Sec12p would be very inefficient in catalyzing Sar1p GDP exchange (Barlowe and Schekman, 1993) and hence unable to support new cycles of Sec23p-GFP recruitment at tER sites.

To determine whether loss of fluorescent puncta in *sec12-4* semi-intact cells resulted from a breakdown of tER sites, or from compromised ER membrane integrity induced by the warm-up, we repeated these reactions replacing GTP with nonhydrolyzable GTPγS. Addition of GTPγS supports COPII vesicle budding, but budding is delayed and overall vesicle production levels reduced (Rexach and Schekman, 1991; Barlowe *et al*., 1994). Therefore, we expected GTPγS to support Sec23p-GFP recruitment to tER sites and then to "lock" Sar1p and COPII coats on ER membranes, producing a delay in vesicle budding as reactions warmed up during imaging. The reactions supplemented with nonhydrolyzable GTPγS rescued the ability of *sec12-4* membranes to retain Sec23p-GFP positive puncta throughout the time course at 23°C. GTPγS also prevented the gradual dissipation of Sec23p-GFP fluorescence in wild-type membranes (Figure 6, B and C). In summary, these results indicate that the *sec12-4* mutation does not dismantle tER sites at 23°C in vitro but that Sec12p activity is required for continuous COPII recruitment and budding from these sites.

Phospholipases Influence COPII Vesicle Budding and Sec23p-GFP Recruitment to tER Sites In Vitro

We next explored lipid requirements for tER site assembly in vitro. The fact that inhibition of fatty acid synthesis induced changes in tER site morphology suggested that COPII coat recruitment depended on the lipid membrane composition. In addition, PI(4)P has been implicated in tER site formation and vesicle budding in vitro, indicating a possible active role for specific phospholipids in ER export (Blumental-Perry *et al*., 2006). We used the cell-free tER site formation and COPII vesicle-budding assays to study specific lipid requirements. The influence of several lipid-binding and lipid-modifying reagents was first assessed in vesicle-budding assays from semi-intact cell membranes. If budding was affected, Sec23p-GFP recruitment to tER sites was monitored under the budding-inhibitory conditions.

A previous report indicated that overexpression of diacylglycerol kinase resulted in negative regulation of Sec13p recruitment to ER exit sites in mammalian cells, suggesting the involvement of diacylglycerol in ER exit site maintenance (Nagaya *et al*., 2002). However, we observed that addition of the diacylglycerol-binding C1b domain had no effect on vesicle budding at 30 μM in vitro, although this concentration of C1b domain partially inhibited the fusion of COPII vesicles with Golgi membranes (Lorente-Rodriguez and Barlowe, unpublished data). The ergosterol-extracting reagent methyl-β-cyclodextran adversely affected vesicle budding at 16 mM but did not influence Sec23p-GFP recruitment to tER sites in vitro (data not shown), in accord with our in vivo observations after lovastatin treatment and consistent with previous findings in mammalian cells (Runz *et al*., 2006). Surprisingly, we were unable to detect any specific inhibition of COPII vesicle budding from *S. cerevisiae* semi-intact cells in the presence of the MBP-Fapp1-PH fusion protein up to 20 μM (data not shown). The PH domain of Fapp1 specifically binds to PI(4)P (Dowler *et al*., 2000), and concentrations of PH domain as low as 5 μM effectively inhibited fusion of ER-derived vesicles with Golgi membranes (Lorente-Rodriguez and Barlowe, unpublished data). Therefore, the observed lack of inhibition was probably not due to insufficient levels of MBP-Fapp1-PH. Although this result contrasted previous findings in mammalian cells that suggested a role for PI(4)P at tER sites (Blumental-Perry *et al*., 2006) other studies have suggested that PI(4)P does not regulate ER export in yeast (Audhya *et al*., 2000). Moreover, we did not detect alterations in tER site structures when Sec13-GFP was imaged in a *pik1-83* mutant (Lorente-Rodriguez and Barlowe, unpublished data), which is deficient in a PI 4-kinase and displays secretion defects and Golgi membrane accumulation (Hendricks *et al*., 1999; Audhya *et al*., 2000), or in a *sac1*Δ strain (Supplemental Table S1), which lacks an ER localized phosphatidylinositol phosphatase and displays elevated ER levels of PI(4)P (Tahirovic *et al*., 2005). Together, these findings indicate that PI(4)P is not directly involved in COPII-dependent vesicle budding or tER site maintenance in *S. cerevisiae*.

The perturbation of Sec13p and Sec23p distribution in cells treated with cerulenin led us to hypothesize that other ER phospholipids may be involved in COPII-dependent vesicle budding and coat recruitment to tER sites. To assess the role of phospholipid head groups in COPII-dependent vesicle budding, we pretreated semi-intact cell membranes with PC-PLC from *Bacillus cereus*. PC-PLC is a broad-specificity phospholipase that hydrolyzes the phosphate bond of phosphatidylcholine, phosphatidylethanolamine, and phosphatidylserine, with a preference for phosphatidylcholine (Roberts *et al*., 1978; Hergenrother and Martin, 1997; Martin *et al*., 2000; Benfield *et al*., 2007). Hydrolysis results in the production of diacylglycerol and soluble phosphocholine.

Washed membranes containing translocated [^{35}S]glyco-pro-α-factor were incubated on ice with increasing amounts of lipase for 10 min, before the addition of cytosol, ATP regeneration system, and GTP to induce vesicle budding. Budding was inhibited in a dose-dependent manner, with 2 mU of *B. cereus* PC-PLC causing a reduction to background levels (Figure 7A). PC-PLC has been shown to induce shrinkage of large unilamellar phosphatidylcholine liposomes (Holopainen *et al*., 2002). To ensure that the apparent inhibition of vesicle budding did not arise from a loss in ER membrane integrity, protease protection of lumenal [^{35}S]glyco-pro-α-factor from tryptic digestion was assessed (Figure 7B). Treatment with 2 mU of PC-PLC preserved ER integrity but specifically blocked COPII vesicle budding. Based on these observations, we propose that an optimal phospholipid composition in the outer leaflet of ER membranes is critical for efficient COPII budding.

We next tested whether PC-PLC pretreatment influenced tER sites by monitoring in vitro recruitment of Sec23p-GFP to semi-intact membranes by fluorescence microscopy. In control reactions, tER sites were detected upon addition of Sec23p-GFP cytosol and further supplementation with Sar1p increased the intensity of fluorescent puncta (Figure 7E). However, Sec23p-GFP puncta were greatly diminished in membranes pretreated with 2 mU of PC-PLC for 10 min, and the presence of excess Sar1p could not rescue this defect (Figure 7E). In membranes pretreated with PC-PLC, the total fluorescence intensity per cell was reduced below background levels in reactions containing cytosol, and to background levels in the presence of excess wild-type Sar1p (Figure 7G). The percentage of semi-intact cell membranes that produced visible puncta showed similar reductions (Figure 7I). These results indicated that the cleavage of phos-

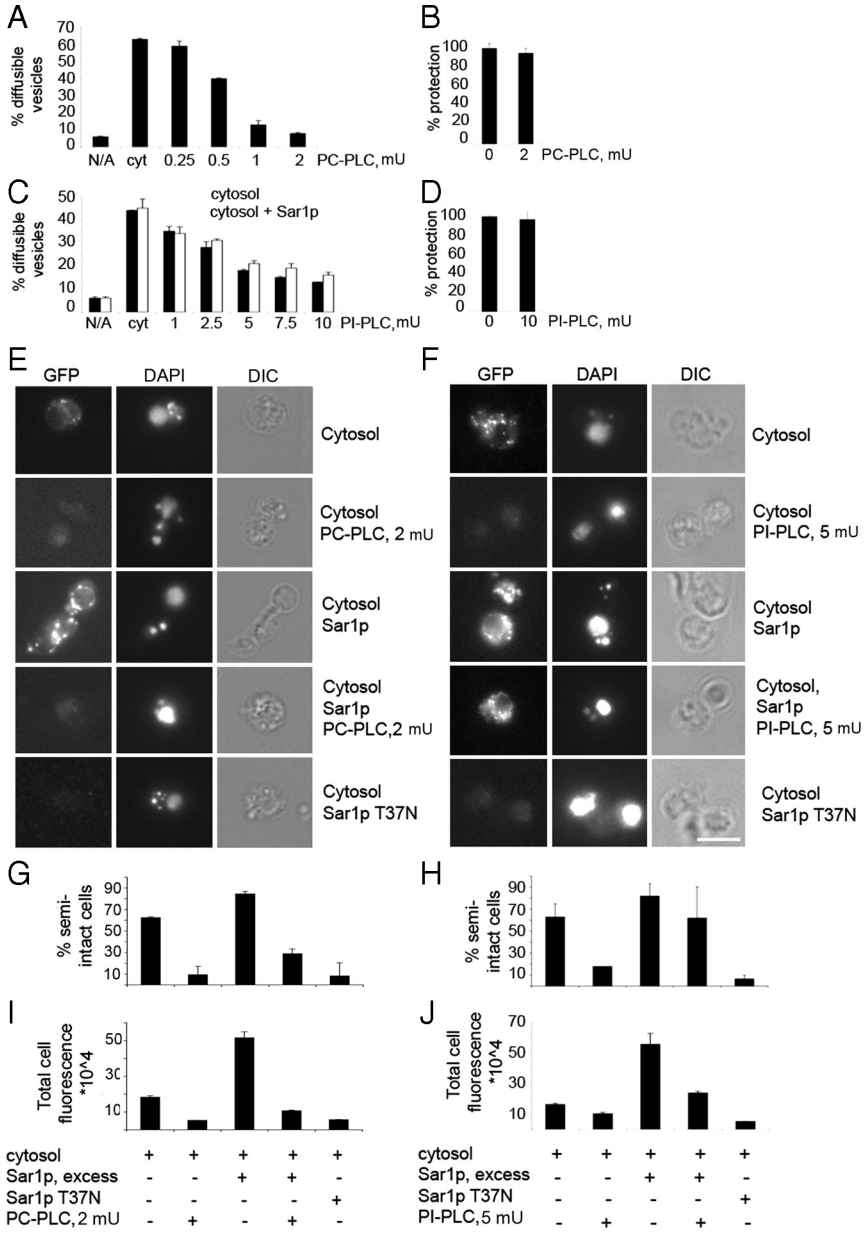

Figure 7. Lipase treatment inhibits Sec23p-GFP recruitment to tER sites in vitro. (A) Washed wild-type (CBY740) semi-intact cell membranes containing [^{35}S]glyco-pro-α-factor were incubated with increasing amounts of PC-PLC at 4°C, supplemented with a Sec23p-GFP cytosol, and budding was measured as described above. (B) ER membrane integrity assessed after treatment with 2 mU of PC-PLC as in A by measuring protease protected [^{35}S]glyco-pro-α-factor as described in *Materials and Methods*. (C) Reactions were assembled as in A except PC-PLC was replaced with the indicated amounts of PI-PLC. (D) Protease protection experiment as in B, replacing PC-PLC with indicated amount of PI-PLC. Note ER integrity was not compromised by lipase treatment. (E) Assembly of Sec23-GFP at tER sites in vitro with washed wild-type semi-intact cell membranes after treatment with PC-PLC as in A. Reactions were supplemented with Sec23p-GFP cytosol, Sar1p, or Sar1p T37N as indicated and incubated at 4°C. (F) Assembly of Sec23p-GFP at tER sites as in E except PC-PLC was replaced with 5 mU of PI-PLC. Note addition of excess Sar1p partially rescues Sec23-GFP recruitment after treatment with PI-PLC but not PC-PLC. (G and H) Quantification of the percentage of semi-intact cells that recruited Sec23p-GFP to puncta, from the images obtained in E and F, respectively. (I and J) Quantification of total fluorescence per semi-intact cell from the images described in E and F, respectively. For plots in G–J, at least 40 cells were analyzed per condition.

pholipid head groups from phosphatidylcholine, and possibly other phospholipids, by PC-PLC inhibited recruitment of Sec23p-GFP to tER sites.

To analyze the potential role of other specific phospholipids in COPII recruitment, membranes were pretreated with a phosphatidylinositol-specific PI-PLC from *B. cereus*. Unlike eukaryotic PI-PLCs, this prokaryotic PI-PLC specifically hydrolyzes the phosphate bond of phosphatidylinositol but not of its phosphorylated derivatives (Volwerk *et al*., 1989; Volwerk *et al*., 1990; Griffith *et al*., 1991; Heinz *et al*., 1998). Membranes were pretreated with PI-PLC on ice for 10 min before the addition of Sec23p-GFP cytosol and remaining reaction components. Vesicle budding was inhibited by 5–10 mU of PI-PLC in the presence and absence of excess Sar1p, without compromising ER integrity (Figure 7, C and D). These inhibitory levels of PI-PLC also blocked Sec23p-GFP recruitment to tER sites in reactions that did not contain additional Sar1p (Figure 7F). Total cell fluorescence and the percentage of semi-intact cells that produced Sec23p-GFP positive puncta decreased in the PI-PLC–treated membranes (Figure 7, H and J). Surprisingly, the addition of excess Sar1p to the recruitment assay partially restored the formation of Sec23p-GFP fluorescent puncta (Figure 7, F, H, and J). These data show that even though PI-PLC greatly reduced the efficiency of Sec23p-GFP recruitment to tER sites, the essential components of the tER site scaffold were not destroyed by the PI-PLC specific treatment. In contrast, the broader specificity PC-PLC completely blocked budding and formation of Sec23p-GFP puncta on ER membranes even in reactions containing elevated Sar1p concentrations.

These results indicate that an optimal lipid composition of ER membranes is critical for efficient recruitment of COPII proteins to tER sites and subsequent vesicle budding. Inhibition is presumably due to reduction of specific phospholipids head groups and/or generation of diacylglycerol in membranes. This altered lipid composition seemed to decrease binding of Sar1p and Sec23/24 complex to tER sites. Increased Sar1p levels after PI-PLC treatment restored

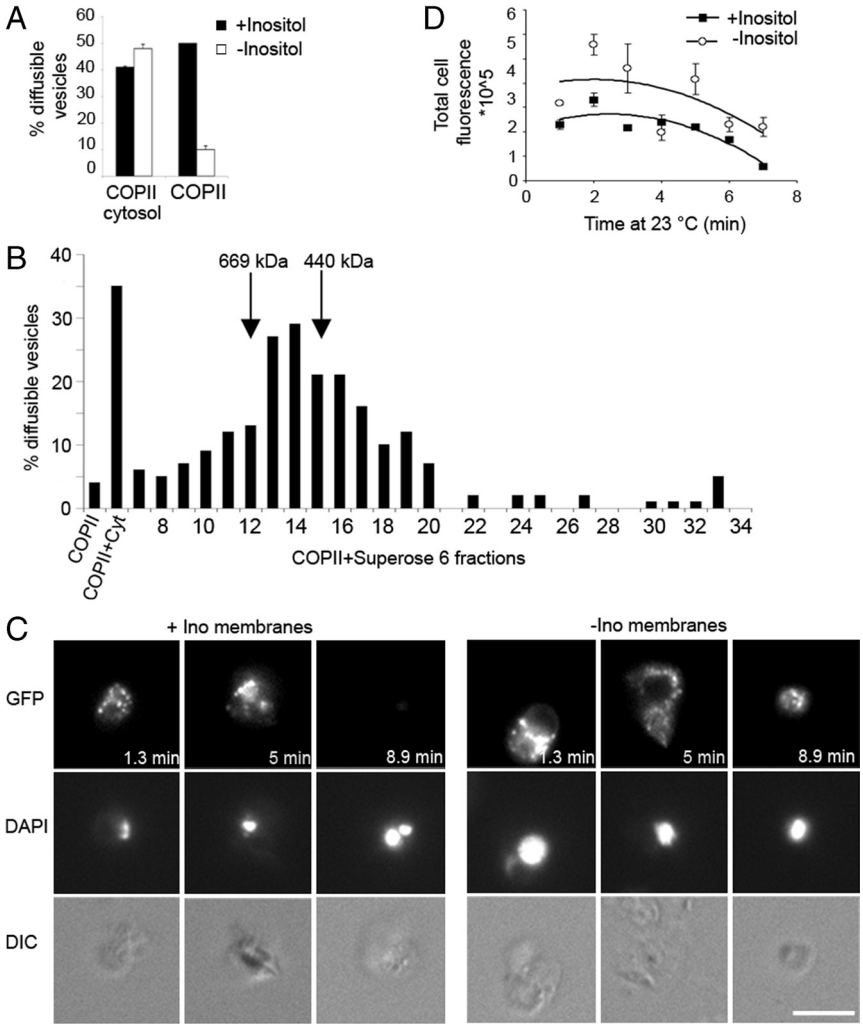

Figure 8. Inositol starved semi-intact cells assemble Sec23p-GFP at tER sites but require cytosol to bud vesicles. (A) Wild-type semi-intact cells grown with or without 75 μM inositol, were assessed in COPII-budding assays in the presence of COPII proteins alone or COPII plus cytosol. Note efficient budding requires cytosol. (B) Wild-type (CBY740) cytosol was fractionated on a Superose 6 column, and 12 μl of each fraction was added to COPII proteins to test stimulation of vesicle budding from inositol-starved membranes. (C) Assembly of Sec23-GFP at tER sites using inositol-starved and unstarved semi-intact cell membranes plus purified Sec23p-GFP/Sec24p complex, Sar1p, and Sec13/Sec31 complex. Reactions were assembled on ice, warmed up to 23°C, and then imaged continuously for ~9 min. Note that both starved and unstarved membranes recruit Sec23p-GFP to tER structures with the minimal set of COPII proteins. (D) Plot showing quantification of total florescence intensity per semi-intact cell from the images obtained in C. At least seven cells were analyzed per condition at each time point.

Sec23/24 subunit binding. Negative membrane curvature induced by removal of phospholipid head groups (Allan *et al*., 1978) could explain the inhibition of COPII-dependent membrane deformation after PI-PLC treatment. Regarding treatment with the broad specificity PC-PLC, the dramatically altered lipid composition may disrupt tER site scaffolds.

COPII Vesicle Budding, but Not Sec23p-GFP Recruitment, Is Inhibited in Membranes Containing Low Levels of PI

Removal of PI by PI-PLC from semi-intact cell membranes blocked vesicle budding and reduced COPII coat recruitment in vitro. In vivo studies on PI requirements for tER site structure were investigated in mutant strains (*pis1* and *ino1*Δ) under conditions that depleted PI levels (Supplemental Table S1). We found that PI-depleted cells ruptured (took up methylene blue) before significant alterations in Sec13-GFP distribution were observed. Unfortunately, these experiments are inconclusive because PI could still be required at tER sites but depletion first affects other essential cellular requirements. Therefore, in vitro approaches were pursued to further investigate the involvement of PI in tER site organization and vesicle budding. Wild-type *S. cerevisiae* cells starved for inositol exhibit a four- to fivefold decrease in total PI content, whereas other phospholipid and diacylglycerol levels are modestly affected (Gaspar *et al*., 2006). It has been reported previously that addition of purified Sar1p, Sec23/24, and Sec13/31 was not sufficient to drive COPII vesicle budding from semi-intact cells that were starved for inositol (Doering and Schekman, 1996). However, ER-derived vesicles could be produced from inositol-starved membranes in the presence of a crude cytosol fraction. These findings indicate that membranes low in PI require additional cytosolic factor(s) to stimulate efficient budding and suggest that suboptimal PI levels may alter COPII budding at tER sites.

To assess tER site morphology and COPII budding under reduced PI concentrations, wild-type cells were grown in synthetic medium lacking inositol, or supplemented with 75 μM inositol as a control. Starved semi-intact cell membranes produced COPII-coated vesicles efficiently in the presence of cytosol, but not with purified COPII proteins alone (Figure 8A). The budding defect was specifically attributed to inositol starvation because the cells grown in medium supplemented with inositol were competent for budding in the presence of purified COPII proteins (Figure 8A). Whole cytosol was fractionated on a Superose 6 column to establish the approximate size of the complementing factors(s). Vesicle-budding activity in starved membranes supplemented with purified COPII coat components was restored by fractions 12–15 (Figure 8B). This corresponded to the size of 440–670 kDa, suggesting that the complementing activity is

a multimolecular protein complex. Further work to identify the factors(s) responsible for this activity is in progress.

To test whether starved membranes were competent to recruit Sec23p-GFP to tER sites in the absence of this complementing cytosolic factor(s), Sec23p–GFP/Sec24p complex was purified following the same procedure as for the native complex. This purified Sec23p–GFP/Sec24p complex supported [^{35}S]gpαf budding from standard ER membranes in the presence of Sar1p and Sec13/31p (data not shown). Purified Sec23p–GFP/Sec24p complex was then used in cell free tER site assembly assays in reactions containing washed semi-intact cell membranes and purified Sar1p and Sec13/31 complex. Our data showed that semi-intact cells grown in the presence or absence of inositol were equally competent in forming Sec23p-GFP fluorescent puncta (Figure 8, C and D). This finding also demonstrated that the minimal COPII proteins (Sar1p, Sec23/24, and Sec13/31) are sufficient for assembly at tER sites. However, we observed that inositol starved membranes incubated with the purified set of COPII proteins retained fluorescent puncta for longer times than inositol-rich membranes when incubated at 23°C (Figure 8D), presumably due to reduced vesicle budding under the inositol-starved condition.

Together, these results indicate that low levels of PI produce a block in vesicle budding from the ER when reactions are supplied with the purified set of COPII proteins. However, tER sites in these inositol-starved cells can functionally recruit Sec23p-GFP and are then stalled at the vesicle-budding stage until additional cytosolic factor(s) are provided. ER membranes with reduced PI levels may depend on additional cytosolic factors to efficiently polymerize COPII coat subunits at tER sites or to promote membrane deformation and vesicle fission events.

DISCUSSION

In this study, we characterized the punctate structures marked by GFP-tagged COPII proteins in *S. cerevisiae* and conclude that these structures represent small tER sites. The COPII labeled structures localize to perinuclear and peripheral elements of ER membranes and display dynamic properties that have been reported for tER sites in other species (Rossanese *et al*., 1999; Forster *et al*., 2006). A recent report has also documented that specific secretory cargo colocalize to Sec13p-GFP marked ER exit sites in *S. cerevisiae* and that *sec12-4* and *sec16-2* mutations alter Sec13p-GFP distribution (Castillon *et al*., 2009). Here, we investigated the protein and lipid requirements for maintenance of functional tER sites through in vivo and in vitro approaches. Our results indicate that specific proteins required for COPII vesicle budding also participate in maintaining tER site structures and that ongoing fatty acid synthesis is required for tER site structure and function. Surprisingly, tER site structures persisted through relatively harsh in vivo and in vitro treatments in which COPII vesicle budding was strongly inhibited. These findings suggest that tER site structures are stable elements and are assembled on an underlying protein/lipid scaffold.

A subset of proteins required for COPII vesicle budding were specifically required to maintain normal tER site structures in vivo. The strongest phenotypes were produced when *sec12-4* and *sec16-2* mutants were shifted to restrictive temperatures. Under these conditions GFP-labeled tER sites did not simply disappear, but instead were observed to cluster into large structures. Intermediate sized puncta were also observed to accumulate in the *sec23-1*, *sec24-11*, and *sec13-1*–budding mutants. Interestingly, the pronounced collapse of tER sites in *sec12-4* and *sec16-2* strains could be rescued by inhibition of protein synthesis, suggesting that accumulated cargo in budding-arrested cells contributed to the appearance of these large COPII aggregates. However, breakdown of tER site morphology in *sec12-4* and *sec16-2* mutants cannot be attributed merely to an accumulation of secretory cargo because other mutants in which ER export is arrested (e.g., *yip1-4*, *uso1-1*, *sed5-1*, and *sec18-1*) retained wild-type–like tER sites. Instead it seems that a failure to properly coordinate coat assembly with incorporation of nascent secretory proteins into tER sites leads to a collapse of normal tER structures.

We speculate that misregulation of the Sar1p GTPase, which governs COPII assembly, could produce the aggregated tER sites observed in this subset of ER–Golgi mutants. Studies on COPII assembly mechanisms in reconstituted proteoliposomes (Sato and Nakano, 2005) indicated that Sar1-GTP dependent binding of Sec23/24 complex to membranes is stabilized through interactions with specific cargo proteins and that repeated cycles of Sec12p-dependent GDP-GTP exchange on Sar1p during coat assembly permit efficient sorting of cargo proteins into COPII vesicles. Therefore, mutations that interfere with the Sar1p GTPase cycle could prevent the COPII machinery from proper kinetic sampling of cargo. In this regard, Sec12p and Sec16p act early in the GTPase cycle to activate and recruit Sar1p to tER sites (Barlowe and Schekman, 1993; Supek *et al*., 2002; Futai *et al*., 2004; Ivan *et al*., 2008). The Sec23/Sec24 and Sec13/31 complexes are also known to influence Sar1p GTPase activity (Yoshihisa *et al*., 1993; Antonny *et al*., 2001). Thus, misregulation of the Sar1p GTPase cycle in these mutant strains, combined with an accumulation of secretory cargo at tER sites, may cause subunits of the COPII complex to irreversibly engage secretory proteins and produce cargo-dependent aggregation of tER sites. In contrast, ER–Golgi mutants that produce an accumulation of secretory cargo in the ER but do not directly interfere with the Sar1p-dependent sorting cycle seem to maintain dispersed tER sites. For example the *yip1-4* mutation, which inhibits COPII budding at restrictive temperatures, did not affect tER site morphology. We hypothesize that Yip1p acts in a very late stage of vesicle budding, after coat polymerization and possibly in vesicle scission (Heidtman *et al*., 2003). Therefore, Yip1p may also not directly influence Sar1p-dependent cargo sorting. Based on these findings, we suggest that the terminal phenotype of misregulated ER export in COPII assembly mutants is distinct from stalled ER export in post-COPII assembly blocks.

Fluorescence microscopy studies in cultured mammalian cell lines by using the GTP-restricted form of Sar1 (Sar1-H79G) are consistent with our proposal regarding misregulation of Sar1p. Expression of Sar1-H79G causes Sec13p clusters to form in juxtanuclear regions in mammalian cells (Ward *et al*., 2001; Yoshimura *et al*., 2004). Moreover, these clusters contain Sec24 protein, secretory cargo, and are continuous with the ER (Stephens and Pepperkok, 2004). Recent reports also indicate that Sec16 localizes to these Sar1-H79G induced clusters (Watson *et al*., 2006). Interestingly, a reduction in Sec16 expression levels in cultured cell lines generally causes an apparent dispersal of COPII-labeled tER structures (Watson *et al*., 2006; Watson *et al*., 2006; Iinuma *et al*., 2007), with some clustering documented previously (Bhattacharyya and Glick, 2007). We also note that a *sec16* mutation isolated in *P. pastoris* produced dispersed tER sites and apparently not large clusters of COPII-positive structures (Connerly *et al*., 2005). It is not clear why some loss of function Sec16 conditions are distinct from the *sec16-2* mutation in *S. cerevisiae* which we observed to induce aggregation of tER sites. These results may be explained if the

sec16-2 mutation produced a partially functional protein that could organize COPII assembly but was deficient in regulation of the Sar1p GTPase cycle at restrictive temperatures. Regardless, Sec16p seems to play a central role in maintaining tER sites and may form an underlying scaffold for tER structures (Supek *et al*., 2002; Connerly *et al*., 2005; Watson *et al*., 2006; Bhattacharyya and Glick, 2007; Ivan *et al*., 2008; Hughes *et al*., 2009).

Investigation of specific lipid requirements for tER site structure and function indicated that yeast tER sites can tolerate major changes in membrane lipid composition. Reduction of sterol and ceramide synthesis to levels that inhibited growth did not produce detectable changes in GFP-marked tER site structures. We note that studies on sterol depleted HeLa cells revealed minor influences on steady-state distribution of Sec23p at tER sites but a significant delay in secretory protein export from the ER and a reduced turnover rate of Sec23p at ER exit sites (Runz *et al*., 2006). Yeast tER sites also tolerated significant changes in the levels of PI in vivo, because tER site morphology remained unchanged in wild-type cells grown in synthetic medium lacking inositol, a condition that was shown to decrease total cellular PI levels four- to fivefold (Gaspar *et al*., 2006), or when PI synthesis was inhibited (Supplemental Table S1). These findings suggest that when a specific lipid biosynthetic pathway is compromised, other pathways can be adjusted to compensate. However, complete inhibition of de novo phospholipid synthesis with cerulenin treatment blocked ER–Golgi trafficking and strikingly altered tER site morphology, suggesting that proper COPII assembly and vesicle budding require a constant supply of newly synthesized phospholipids. It is not known whether constant production of phospholipids is required for Sar1p-dependent recruitment of coat subunits and/or for membrane deformation and vesicle fission. Further studies will be required to determine the mechanism by which depletion of newly synthesized phospholipids blocks budding from tER sites.

We established an in vitro assay in yeast semi-intact cells to monitor recruitment of Sec23p-GFP to tER sites that depended on the minimal set of COPII proteins, GTP, and ATP regeneration system. A similar assay after immunofluorescence staining of Sec24p was developed in mammalian cells to identify new factors that stimulate COPII assembly at tER sites (Kapetanovich *et al*., 2005). The assay in yeast semi-intact cells allowed us to monitor the requirements for recruitment and dissociation of Sec23p-GFP to tER sites in real time. Moreover, these reactions could be performed in parallel with [^{35}S]gpαf budding assays to quantify levels of COPII-dependent export. We observed that when reactions were warmed to temperatures that permitted COPII budding, tER sites gradually lost Sec23p-GFP fluorescence over an ~10-min time interval. We speculate that in vitro, without ongoing protein translation and without retrograde transport back from post-ER compartments, the ER quickly becomes depleted of cargo proteins and leaves no export signals at tER sites to stably bind COPII components (Sato and Nakano, 2005). We note that addition of GTPγS preserved Sec23p-GFP puncta for extended periods, presumably due to inhibition of vesicle budding with COPII coats locked on to cargo at tER sites.

In *sec12-4* semi-intact cells, we observed efficient recruitment of Sec23-GFP to tER sites on ice, but upon warm up to budding temperatures, tER fluorescence declined at a faster rate than in wild-type semi-intact cell membranes. These results suggest that after an initial round of budding the mutant Sec12p protein could not efficiently activate Sar1p at tER sites to initiate additional rounds of budding (Rexach and Schekman, 1991; d'Enfert *et al*., 1991; Barlowe and Schekman, 1993). Addition of GTPγS preserved Sec23-GFP fluorescence at tER sites over a prolonged period in the *sec12-4* semi-intact cells. However, tER sites did not collapse into the single large structures we observed in vivo. We speculate that without ongoing protein translation and retrograde transport that the large cargo-dependent aggregates observed in vivo do not form in this cell-free assay.

We also assessed lipid requirements for tER site assembly in vitro and did not detect specific requirements for sterols or PI(4)P. However, a requirement for bulk membrane phospholipids in maintenance of tER site structures as observed in vivo was confirmed in vitro. Pretreatment with PC-PLC, a broad specificity phospholipase, strongly inhibited COPII budding and assembly of Sec23p-GFP at tER sites, even when elevated levels of Sar1p were provided. These results suggest that loss of charged phospholipid head groups after PC-PLC treatment disrupted tER site structures. Treatment with a PI-specific PLC inhibited COPII budding and Sec23p-GFP assembly at tER sites; however, addition of excess Sar1p could restore assembly of Sec23p-GFP–positive structures. The phospholipid composition of yeast microsomal membranes is ~10% PI and 50% PC (Zinser and Daum, 1995); therefore, we speculate that the consequence of PC-PLC treatment has a much greater impact on tER site structure and function. The protein components that localize selectively to the tER site scaffold, such as Sec16p, may be dispersed and/or rendered inactive as a result of the cleavage of phospholipids head groups by PC-PLC. Further experiments to examine Sec16p localization after inhibition of fatty acid synthesis and phospholipase treatments should be informative.

The properties of tER sites in inositol starved semi-intact cell membranes were similar to PI-PLC–treated membranes. Under both conditions, Sec23p-GFP could be assembled into tER sites but COPII budding was inhibited. This altered phospholipid composition could block budding at a coat polymerization stage or at vesicle fission. Interestingly, the deficit in vesicle budding from inositol-starved membranes could be restored by supplementing the minimal set of COPII proteins with a cytosolic fraction. Preliminary characterization of the complementing activity showed that the factor was heat labile and fractionated at an apparent molecular mass of ~500 kDa. Our collective results indicate that tER site structure and function depend on specific protein and lipid species. Identification and characterization of the cytosolic factor(s) necessary to stimulate budding from inositol-starved membranes should provide additional molecular insights into the ER export process.

ACKNOWLEDGMENTS

We thank Ben Glick for providing the Sec23p-GFP and Sec13p-GFP constructs, the Cole laboratory for actin antibodies and the Wickner laboratory for anti-GFP antiserum. We are grateful to Bill Wickner, Duane Compton and members of both laboratories for their generous assistance in microscopy. We also thank Christine Bentivoglio and Andres Lorente-Rodriguez for help with experiments and for sharing their unpublished observations. This work was supported by the National Institutes of Health.

REFERENCES

Allan, D., Thomas, P., and Michell, R. H. (1978). Rapid transbilayer diffusion of 1,2-diacylglycerol and its relevance to control of membrane curvature. Nature *276*, 289–290.

Antonny, B., Madden, D., Hamamoto, S., Orci, L., and Schekman, R. (2001). Dynamics of the COPII coat with GTP and stable analogues. Nat. Cell Biol. *3*, 531–537.

Audhya, A., Foti, M., and Emr, S. D. (2000). Distinct roles for the yeast phosphatidylinositol 4-kinases, Stt4p and Pik1p, in secretion, cell growth, and organelle membrane dynamics. Mol. Biol. Cell *11*, 2673–2689.

Baker, D., Hicke, L., Rexach, M., Schleyer, M., and Schekman, R. (1988). Reconstitution of SEC gene product-dependent intercompartmental protein transport. Cell *54*, 335–344.

Bannykh, S. I., Rowe, T., and Balch, W. E. (1996). The organization of endoplasmic reticulum export complexes. J. Cell Biol. *135*, 19–35.

Bevis, B. J., Hammond, A. T., Reinke, C. A., and Glick, B. S. (2002). De novo formation of transitional ER sites and Golgi structures in Pichia pastoris. Nat. Cell Biol. *4*, 750–756.

Bhattacharyya, D., and Glick, B. S. (2007). Two mammalian Sec16 homologues have nonredundant functions in endoplasmic reticulum (ER) export and transitional ER organization. Mol. Biol. Cell *18*, 839–849.

Barlowe, C. (1997). Coupled ER to Golgi transport reconstituted with purified cytosolic proteins. J. Cell Biol. *139*, 1097–1108.

Barlowe, C., Orci, L., Yeung, T., Hosobuchi, M., Hamamoto, S., Salama, N., Rexach, M. F., Ravazzola, M., Amherdt, M., and Schekman, R. (1994). COPII: a membrane coat formed by Sec proteins that drive vesicle budding from the endoplasmic reticulum. Cell *77*, 895–907.

Barlowe, C., and Schekman, R. (1993). SEC12 encodes a guanine-nucleotide-exchange factor essential for transport vesicle budding from the ER. Nature *365*, 347–349.

Belden, W. J., and Barlowe, C. (1996). Erv25p, a component of COPII-coated vesicles, forms a complex with Emp24p that is required for efficient endoplasmic reticulum to Golgi transport. J. Biol. Chem. *271*, 26939–26946.

Benfield, A. P., Goodey, N. M., Phillips, L. T., and Martin, S. F. (2007). Structural studies examining the substrate specificity profiles of PC-PLC(Bc) protein variants. Arch. Biochem. Biophys. *460*, 41–47.

Blumental-Perry, A., Haney, C. J., Weixel, K. M., Watkins, S. C., Weisz, O. A., and Aridor, M. (2006). Phosphatidylinositol 4-phosphate formation at ER exit sites regulates ER export. Dev. Cell *11*, 671–682.

Calero, M., Chen, C. Z., Zhu, W., Winand, N., Havas, K. A., Gilbert, P. M., Burd, C. G., and Collins, R. N. (2003). Dual prenylation is required for Rab protein localization and function. Mol. Biol. Cell *14*, 1852–1867.

Cao, X., and Barlowe, C. (2000). Asymmetric requirements for a Rab GTPase and SNARE proteins in fusion of COPII vesicles with acceptor membranes. J. Cell Biol. *149*, 55–66.

Castillon, G. A., Watanabe, R., Taylor, M., Schwabe, T. M., and Riezman, H. (2009). Concentration of GPI-anchored proteins upon ER exit in yeast. Traffic *10*, 186–200.

Connerly, P. L., Esaki, M., Montegna, E. A., Strongin, D. E., Levi, S., Soderholm, J., and Glick, B. S. (2005). Sec16 is a determinant of transitional ER organization. Curr. Biol. *15*, 1439–1447.

d'Enfert, C., Wuestehube, L. J., Lila, T., and Schekman, R. (1991). Sec12p-dependent membrane binding of the small GTP-binding protein Sar1p promotes formation of transport vesicles from the ER. J. Cell Biol. *114*, 663–670.

Doering, T. L., and Schekman, R. (1996). GPI anchor attachment is required for Gas1p transport from the endoplasmic reticulum in COP II vesicles. EMBO J. *15*, 182–191.

Dowler, S., Currie, R. A., Campbell, D. G., Deak, M., Kular, G., Downes, C. P., and Alessi, D. R. (2000). Identification of pleckstrin-homology-domain-containing proteins with novel phosphoinositide-binding specificities. Biochem. J. *351*, 19–31.

Farhan, H., Weiss, M., Tani, K., Kaufman, R. J., and Hauri, H. P. (2008). Adaptation of endoplasmic reticulum exit sites to acute and chronic increases in cargo load. EMBO J. *27*, 2043–2054.

Forster, R., Weiss, M., Zimmermann, T., Reynaud, E. G., Verissimo, F., Stephens, D. J., and Pepperkok, R. (2006). Secretory cargo regulates the turnover of COPII subunits at single ER exit sites. Curr. Biol. *16*, 173–179.

Futai, E., Hamamoto, S., Orci, L., and Schekman, R. (2004). GTP/GDP exchange by Sec12p enables COPII vesicle bud formation on synthetic liposomes. EMBO J. *23*, 4146–4155.

Gaspar, M. L., Aregullin, M. A., Jesch, S. A., and Henry, S. A. (2006). Inositol induces a profound alteration in the pattern and rate of synthesis and turnover of membrane lipids in *Saccharomyces cerevisiae*. J. Biol. Chem. *281*, 22773–22785.

Griffith, O. H., Volwerk, J. J., and Kuppe, A. (1991). Phosphatidylinositol-specific phospholipases C from *Bacillus* cereus and *Bacillus thuringiensis*. Methods Enzymol. *197*, 493–502.

Hammond, A. T., and Glick, B. S. (2000). Dynamics of transitional endoplasmic reticulum sites in vertebrate cells. Mol. Biol. Cell *11*, 3013–3030.

Heidtman, M., Chen, C. Z., Collins, R. N., and Barlowe, C. (2003). A role for Yip1p in COPII vesicle biogenesis. J. Cell Biol. *163*, 57–69.

Heinz, D. W., Essen, L. O., and Williams, R. L. (1998). Structural and mechanistic comparison of prokaryotic and eukaryotic phosphoinositide-specific phospholipases C. J. Mol. Biol. *275*, 635–650.

Hendricks, K. B., Wang, B., Schnieders, E., and Thorner, J. (1999). Yeast homologue of neuronal frequenin is a regulator of phosphatidylinositol-4-OH kinase. Nat. Cell Biol. *1*, 234–241.

Hicke, L., and Schekman, R. (1989). Yeast Sec23p acts in the cytoplasm to promote protein transport from the endoplasmic reticulum to the Golgi complex in vivo and in vitro. EMBO J. *8*, 1677–1684.

Holopainen, J. M., Angelova, M. I., Söderlund, T., and Kinnunen, P. K. (2002). Macroscopic consequences of the action of phospholipase C on giant unilamellar liposomes. Biophys. J. *83*, 932–943.

Hergenrother, P. J., and Martin, S. F. (1997). Determination of the kinetic parameters for phospholipase C (*Bacillus cereus*) on different phospholipid substrates using a chromogenic assay based on the quantitation of inorganic phosphate. Anal. Biochem. *251*, 45–49.

Hughes, H., *et al*. (2009). Organisation of human ER-exit sites: requirements for the localisation of Sec16 to transitional ER. J. Cell Sci. *122*, 2924–2934.

Iinuma, T., Shiga, A., Nakamoto, K., O'Brien, M. B., Aridor, M., Arimitsu, N., Tagaya, M., and Tani, K. (2007). Mammalian Sec16/p250 plays a role in membrane traffic from the endoplasmic reticulum. *J. Biol. Chem. 282*, 17632–17639.

Inokoshi, J., Tomoda, H., Hashimoto, H., Watanabe, A., Takeshima, H., and Omura, S. (1994). Cerulenin-resistant mutants of *Saccharomyces cerevisiae* with an altered fatty acid synthase gene. Mol. Gen. Genet. *244*, 90–96.

Ito, H., Fukuda, Y., Murata, K., and Kimura, A. (1983). Transformation of intact yeast cells treated with alkali cations. *J. Bacteriol. 153*, 163–168.

Ivan, V., de Voer, G., Xanthakis, D., Spoorendonk, K. M., Kondylis, V., and Rabouille, C. (2008). Drosophila Sec16 mediates the biogenesis of tER sites upstream of Sar1 through an arginine-rich motif. Mol. Biol. Cell *19*, 4352–4365.

Jesch, S. A., Zhao, X., Wells, M. T., and Henry, S. A. (2005). Genome-wide analysis reveals inositol, not choline, as the major effector of Ino2p-Ino4p and unfolded protein response target gene expression in yeast. J. Biol. Chem. *280*, 9106–9118.

Kaiser, C. A., and Schekman, R. (1990). Distinct sets of SEC genes govern transport vesicle formation and fusion early in the secretory pathway. Cell *61*, 723–733.

Kapetanovich, L., Baughman, C., and Lee, T. H. (2005). Nm23H2 facilitates coat protein complex II assembly and endoplasmic reticulum export in mammalian cells. Mol. Biol. Cell, *16*, 835–848.

Kirk, S. J., and Ward, T. H. (2007). COPII under the microscope. Semin. Cell Dev. Biol. *18*, 435–447.

Kondylis, V., and Rabouille, C. (2003). A novel role for dp115 in the organization of tER sites in *Drosophila*. J. Cell Biol. *162*, 185–198.

Kuehn, M. J., Herrmann, J. M., and Schekman, R. (1998). COPII-cargo interactions direct protein sorting into ER-derived transport vesicles. Nature *391*, 187–190.

Kuge, O., Dascher, C., Orci, L., Rowe, T., Amherdt, M., Plutner, H., Ravazzola, M., Tanigawa, G., Rothman, J. E., and Balch, W. E. (1994). Sar1 promotes vesicle budding from the endoplasmic reticulum but not Golgi compartments. J. Cell Biol. *125*, 51–65.

Lee, M. C., Miller, E. A., Goldberg, J., Orci, L., and Schekman, R. (2004). Bi-directional protein transport between the ER and Golgi. Annu. Rev. Cell Dev. Biol. *20*, 87–123.

Lewis, M. J., and Pelham, H. R. (1996). SNARE-mediated retrograde traffic from the Golgi complex to the endoplasmic reticulum. Cell *85*, 205–215.

Longtine, M. S., McKenzie, A., III, Demarini, D. J., Shah, N. G., Wach, A., Brachat, A., Philippsen, P., and Pringle, J. R. (1998). Additional modules for versatile and economical PCR-based gene deletion and modification in *Saccharomyces cerevisiae*. Yeast *14*, 953–961.

Losev, E., Reinke, C. A., Jellen, J., Strongin, D. E., Bevis, B. J., and Glick, B. S. (2006). Golgi maturation in living yeast. Nature *441*, 1002–1006.

Martin, S. F., Follows, B. C., Hergenrother, P. J., and Trotter, B. K. (2000). The choline binding site of phospholipase C (*Bacillus cereus*): insights into substrate specificity. Biochemistry *39*, 3410–3415.

Matsuoka, K., Schekman, R., Orci, L., and Heuser, J. E. (2001). Surface structure of the COPIIcoated vesicle. Proc. Natl. Acad. Sci. USA *98*, 13705–13709.

Miller, E. A., Beilharz, T. H., Malkus, P. N., Lee, M. C., and Hamamoto, S. (2003). Multiple cargo binding sites on the COPII subunit Sec24p ensure capture of diverse membrane proteins into transport vesicles. Cell *114*, 497–509.

Morin-Ganet, M. N., Rambourg, A., Deitz, S. B., Franzusoff, A., and Képès, F. (2000). Morphogenesis and dynamics of the yeast Golgi apparatus. Traffic *1*, 56–68.

Mossessova, E., Bickford, L. C., and Goldberg, J. (2003). SNARE selectivity of the COPII coat. Cell *114*, 483–495.

Nagaya, H., Wada, I., Jia, Y. J., and Kanoh, H. (2002). Diacylglycerol kinase delta suppresses ER-to-Golgi traffic via its SAM and PH domains. Mol. Biol. Cell *13*, 302–316.

Nakajima, H., Hirata, A., Ogawa, Y., Yonehara, T., Yoda, K., and Yamasaki, M. (1991). A cytoskeleton-related gene, uso1, is required for intracellular protein transport in *Saccharomyces cerevisiae*. J. Cell Biol. *113*, 245–260.

Nakano, A., and Muramatsu, M. (1989). A novel GTP-binding protein, Sar1p, is involved in transport from the endoplasmic reticulum to the Golgi apparatus. J. Cell Biol. *109*, 2677–2691.

Nishikawa, S., and Nakano, A. (1991). The GTP-binding Sar1 protein is localized to the early compartment of the yeast secretory pathway. Biochim. Biophys. Acta *1093*, 135–143.

Nishikawa, S., and Nakano, A. (1993). Identification of a gene required for membrane protein retention in the early secretory pathway. Proc. Natl. Acad. Sci. USA *90*, 8179–8183.

Nomura, S., Horiuchi, T., Omura, S., and Hata, T. (1972). The action mechanism of cerulenin. I. Effect of cerulenin on sterol and fatty acid biosynthesis in yeast. J. Biochem. *71*, 783–796.

Novick, P., Field, C., and Schekman, R. (1980). Identification of 23 complementation groups required for post-translational events in the yeast secretory pathway. Cell *21*, 205–215.

Orci, L., Ravazzola, M., Meda, P., Holcomb, C., Moore, H. P., Hicke, L., and Schekman, R. (1991). Mammalian Sec23p homologue is restricted to the endoplasmic reticulum transitional cytoplasm. Proc. Natl. Acad. Sci. USA *88*, 8611–8615.

Otte, S., Belden, W. J., Heidtman, M., Liu, J., Jensen, O. N., and Barlowe, C. (2001). Erv41p and Erv46p: new components of COPII vesicles involved in transport between the ER and Golgi complex. J. Cell Biol. *152*, 503–518.

Peng, R., De Antoni, A., and Gallwitz, D. (2000). Evidence for overlapping and distinct functions in protein transport of coat protein Sec24p family members. J. Biol. Chem. *275*, 11521–11528.

Powers, J., and Barlowe, C. (2002). Erv14p directs a transmembrane secretory protein into COPII-coated transport vesicles. Mol. Biol. Cell *13*, 880–891.

Rexach, M. F., and Schekman, R. W. (1991). Distinct biochemical requirements for the budding, targeting, and fusion of ER-derived transport vesicles. J. Cell Biol. *114*, 219–229.

Roberts, M. F., Otnaess, A. B., Kensil, C. A., and Dennis, E. A. (1978). The specificity of phospholipase A2 and phospholipase C in a mixed micellar system. J. Biol. Chem. *253*, 1252–1257.

Rossanese, O. W., Soderholm, J., Bevis, B. J., Sears, I. B., O'Connor, J., Williamson, E. K., and Glick, B. S. (1999). Golgi structure correlates with transitional endoplasmic reticulum organization in *Pichia pastoris* and *Saccharomyces cerevisiae*. J. Cell Biol. *145*, 69–81.

Rothblatt, J. A., Deshaies, R. J., Sanders, S. L., Daum, G., and Schekman, R. (1989). Multiple genes are required for proper insertion of secretory proteins into the endoplasmic reticulum in yeast. J. Cell Biol. *109*, 2641–2652.

Runz, H., Miura, K., Weiss, M., and Pepperkok, R. (2006). Sterols regulate ER-export dynamics of secretory cargo protein ts-O45-G. EMBO J. *25*, 2953–2965.

Salama, N. R., Yeung, T., and Schekman, R. W. (1993). The Sec13p complex and reconstitution of vesicle budding from the ER with purified cytosolic proteins. EMBO J. *12*, 4073–4082.

Scarcelli, J. J., Hodge, C. A., and Cole, C. N. (2007). The yeast integral membrane protein Apq12 potentially links membrane dynamics to assembly of nuclear pore complexes. J. Cell Biol. *178*, 799–812.

Soderholm, J., Bhattacharyya, D., Strongin, D., Markovitz, V., Connerly, P. L., Reinke, C. A., and Glick, B. S. (2004). The transitional ER localization mechanism of *Pichia pastoris* Sec12. Dev. Cell *6*, 649–659.

Sato, K., and Nakano, A. (2005). Dissection of COPII subunit-cargo assembly and disassembly kinetics during Sar1p-GTP hydrolysis. Nat. Struct. Mol. Biol. *12*, 167–174.

Stagg, S. M., Gurkan, C., Fowler, P., LaPointe, P., Foss, T. R., Potter, C. S., Carragher, B., and Balch, W. E. (2006). Structure of the Sec13/31 COPII coat cage. Nature *439*, 234–238.

Stephens, D. J. (2003). De novo formation, fusion and fission of mammalian COPII coated endoplasmic reticulum exit sites. EMBO Rep. *4*, 210–217.

Stephens, D. J., Lin-Marq, N., Pagano, A., Pepperkok, R., and Paccaud, J. P. (2000). COPI-coated ER-to-Golgi transport complexes segregate from COPII in close proximity to ER exit sites. J. Cell Sci. *113*, 2177–2185.

Stephens, D. J., and Pepperkok, R. (2004). Differential effects of a GTP-restricted mutant of Sar1p on segregation of cargo during export from the endoplasmic reticulum. J. Cell Sci. *117*, 3635–3644.

Supek, F., Madden, D. T., Hamamoto, S., Orci, L., and Schekman, R. (2002). Sec16p potentiates the action of COPII proteins to bud transport vesicles. J. Cell Biol. *158*, 1029–1038.

Sütterlin, C., Doering, T. L., Schimmöller, F., Schröder, S., and Riezman, H. (1997). Specific requirements for the ER to Golgi transport of GPI-anchored proteins in yeast. J. Cell Sci. *110*, 2703–2714.

Tahirovic, S., Schorr, M., and Mayinger, P. (2005). Regulation of intracellular phosphatidylinositol-4-phosphate by the Sac1 lipid phosphatase. Traffic *6*, 116–130.

Vacaru, A. M., Tafesse, F. G., Ternes, P., Kondylis, V., Hermansson, M., Brouwers, J. F., Somerharju, P., Rabouille, C., and Holthuis, J. C. (2009). Sphingomyelin synthase-related protein SMSr controls ceramide homeostasis in the ER. J. Cell Biol. *185*, 1013–1027.

Volwerk, J. J., Koke, J. A., Wetherwax, P. B., and Griffith, O. H. (1989). Functional characteristics of phosphatidylinositol-specific phospholipases C from *Bacillus cereus* and *Bacillus* thuringiensis. FEMS Microbiol. Lett. *52*, 237–241.

Volwerk, J. J., Shashidhar, M. S., Kuppe, A., and Griffith, O. H. (1990). Phosphatidylinositol-specific phospholipase C from *Bacillus cereus* combines intrinsic phosphotransferase and cyclic phosphodiesterase activities: a 31P NMR study. Biochemistry *29*, 8056–8062.

Ward, T. H., Polishchuk, R. S., Caplan, S., Hirschberg, K., and Lippincott-Schwartz, J. (2001). Maintenance of Golgi structure and function depends on the integrity of ER export. J. Cell Biol. *155*, 557–570.

Watson, P., Townley, A. K., Koka, P., Palmer, K. J., and Stephens, D. J. (2006). Sec16 defines endoplasmic reticulum exit sites and is required for secretory cargo export in mammalian cells. Traffic *7*, 1678–1687.

Weissman, J. T., Plutner, H., and Balch, W. E. (2001). The mammalian guanine nucleotide exchange factor mSec12 is essential for activation of the Sar1 GTPase directing endoplasmic reticulum export. Traffic *2*, 465–475.

Winston, F., Dollard, C., and Ricupero-Hovasse, L. L. (1995). Construction of a set of convenient *Saccharomyces cerevisiae* strains that are isogenic to S288C. Yeast *11*, 53–55.

Wooding, S., and Pelham, H. R. (1998). The dynamics of Golgi protein traffic visualized in living yeast cells. Mol. Biol. Cell *9*, 2667–2680.

Yang, Y. D., Elamawi, R., Bubeck, J., Pepperkok, R., Ritzenthaler, C., and Robinson, D. G. (2005). Dynamics of COPII vesicles and the Golgi apparatus in cultured Nicotiana tabacum BY-2 cells provides evidence for transient association of Golgi stacks with endoplasmic reticulum exit sites. Plant Cell *17*, 1513–1531.

Yoshihisa, T., Barlowe, C., and Schekman, R. (1993). Requirement for a GTPase-activating protein in vesicle budding from the endoplasmic reticulum. Science *259*, 1466–1468.

Yoshimura, S., Yamamoto, A., Misumi, Y., Sohda, M., Barr, F. A., Fujii, G., Shakoori, A., Ohno, H., Mihara, K., and Nakamura, N. (2004). Dynamics of Golgi matrix proteins after the blockage of ER to Golgi transport. J. Biochem. *135*, 201–216.

Zinser, E., and Daum, G. (1995). Isolation and biochemical characterization of organelles from the yeast, *Saccharomyces cerevisiae*. Yeast *11*, 493–536.